NASA CR-159731

NASA

INTERACTION OF HIGH VOLTAGE SURFACES WITH THE SPACE PLASMA

Prepared for

LEWIS RESEARCH CENTER

NATIONAL AERONAUTICS AND SPACE ADMINISTRATION

GRANT NSG 3196

Annual Report

May 1979

Harold R. Kaufman and Raymond S. Robinson
Department of Physics
Colorado State University
Fort Collins, Colorado

1. Report No.	2. Government Accession No.	3. Recipient's Catalog No.
CR-159731		

4. Title and Subtitle	5. Report Date
Interaction of high voltage surfaces with the space plasma	May 1979
	6. Performing Organization Code

7. Author(s)	8. Performing Organization Report No.
Harold R. Kaufman and	

9. Performing Organization Name and Address	10. Work Unit No.
Department of Physics Colorado State University Fort Collins, CO 80523	11. Contract or Grant No. NSG-3196

12. Sponsoring Agency Name and Address	13. Type of Report and Period Covered
National Aeronautics and Space Agency Washington, D.C. 20546	Contractor Report
	14. Sponsoring Agency Code

15. Supplementary Notes

Grant Manager: Norman T. Grier
NASA Lewis Research Center
Cleveland, Ohio 44135

16. Abstract

High voltage solar arrays are desired to provide spacecraft power while optimizing mass and power efficiency. Operating such arrays in the space plasma environment can result in anomalously large currents being collected through insulation defects. Understanding this phenomen was the objective of this research.

Tests were conducted using plasma densities of approximately 10^5-$10^6 cm^{-3}$. Insulating materials tested were polyimide (Dapton), mica and glass. Surface-area effects were found to be substantially reduced from those previously reported at lower plasma densities. The difference in typical plasma density was felt to be the major cause of this change, although a saturation effect may also be involved. At the $10^5/cm^3$ plasma density range of this investigation, surface effects on collection current appear limited to roughly 1 cm from the hole.

A factor of several reduction of collected current was obtained with both surface scribing and a 2 x 2 cm conducting mesh. It appears possible that the effects of surface treatment might be more significant at lower plasma densities.

Effects of repeated tests were also noted, with current collection decreasing with successive tests. Depending on the materials involved, the effect appeared due to either the smoothing of the inside of the insulator hole or the sputtering of insulator on the exposed conductor.

A general conclusion was made from a variety of observations, that the generation of vapor was a major factor in the enhancement of collected current. Because of the importance of vapor generation, future studies should include sample temperature variation.

17. Key Words (Suggested by Author(s))	18. Distribution Statement
Plasma Physics Space Plasma Solar Arrays	Unclassified-Unlimited

19. Security Classif. (of this report)	20. Security Classif. (of this page)	21. No. of Pages	22. Price*
Unclassified	Unclassified		

* For sale by the National Technical Information Service, Springfield, Virginia 22161

NASA-C-168 (Rev. 10-75)

N80-14923

TABLE OF CONTENTS

LIST OF FIGURES

I. INTRODUCTION

The major objective of this research was to investigate the phenomenon of unexpectedly large currents collected by exposed areas of high voltage solar arrays operated in the low density plasma environment of space. For spacecraft operation in the near-earth environment, solar cell arrays constitute the present major source of long term power. High voltage arrays are desired to optimize both spacecraft mass and power efficiency.

The space plasma[1-3] constitutes an important and sometimes critical aspect of the near-earth environment for high voltage solar arrays. Operating such arrays in a plasma environment can result in large currents being collected by any exposed electrode in the array. The obvious solution of using a covering of transparent insulation is at least partially offset by the expectation of defects, either from the manufacturing process or resulting from collisions with micrometeorites.

Early experiments by Cole, Ogawa, and Sellen showed that positive electrodes behind pinhole openings in insulating sheets could collect electron currents far in excess of what would be expected from the hole area and simple electrostatic probe theory.[4] This result was subsequently verified by other investigators for several plasma environments.[5-8] At high enough plasma densities and electron currents, the current collection process degrades into a visible arc, in which electrode and/or insulator material is rapidly vaporized to further enhance conduction. At low plasma densities, the anomalously large electron currents are collected in the absence of a visible arc, and appear to be associated with a nearly nondestructive surface phenomenon. In the

absence of a visible arc, the electron current is typically observed to rise steeply between 100 and 1000 volts, then to level out at high voltages. The maximum current at high voltage appears, from previous investigations, to depend primarily on the plasma density and the area of the insulating surface surrounding the pinhole.

II. APPARATUS AND PROCEDURE

Robert P. Stillwell

Vacuum Facility

The experiments were conducted in a 45 cm diameter bell jar. An argon hollow cathode was used as the source of the plasma in the bell jar facility. As indicated in Fig. 2-1, the hollow cathode was centrally located and directed upward. The anode was cylindrical and perforated. The only source of argon gas in the bell jar was the flow through the hollow cathode, which was between 100 to 600 mA equivalent for discharge currents of 0.1 to 2.0 A. A conical baffle was placed over the open end of the cylindrical anode, to provide the desired range of plasma densities. By varying hollow cathode discharge currents and mass flow, a controllable and reproducible plasma environment was generated.

Typical plasma characteristics used for the experiments are as follows:

background pressure, $P \approx 1 - 2 \times 10^{-4}$ Torr,

electron temperature, $T_e \approx 2 - 8$ eV,

electron density, $n \approx 10^5 - 10^6$ cm^{-3},

plasma potential, $V_p \approx 20 - 25$ V.

Measurement of Plasma Characteristics

A 1.3 cm diameter spherical probe was used to measure most of the plasma characteristics (see Appendix A). Initially, cylindrical probes of various geometries were tried. A cylindrical probe of 5 cm length proved satisfactory down to plasma densities of 10^8 cm^{-3}. Below this density, the plasma Debye length dictates a probe length which approaches

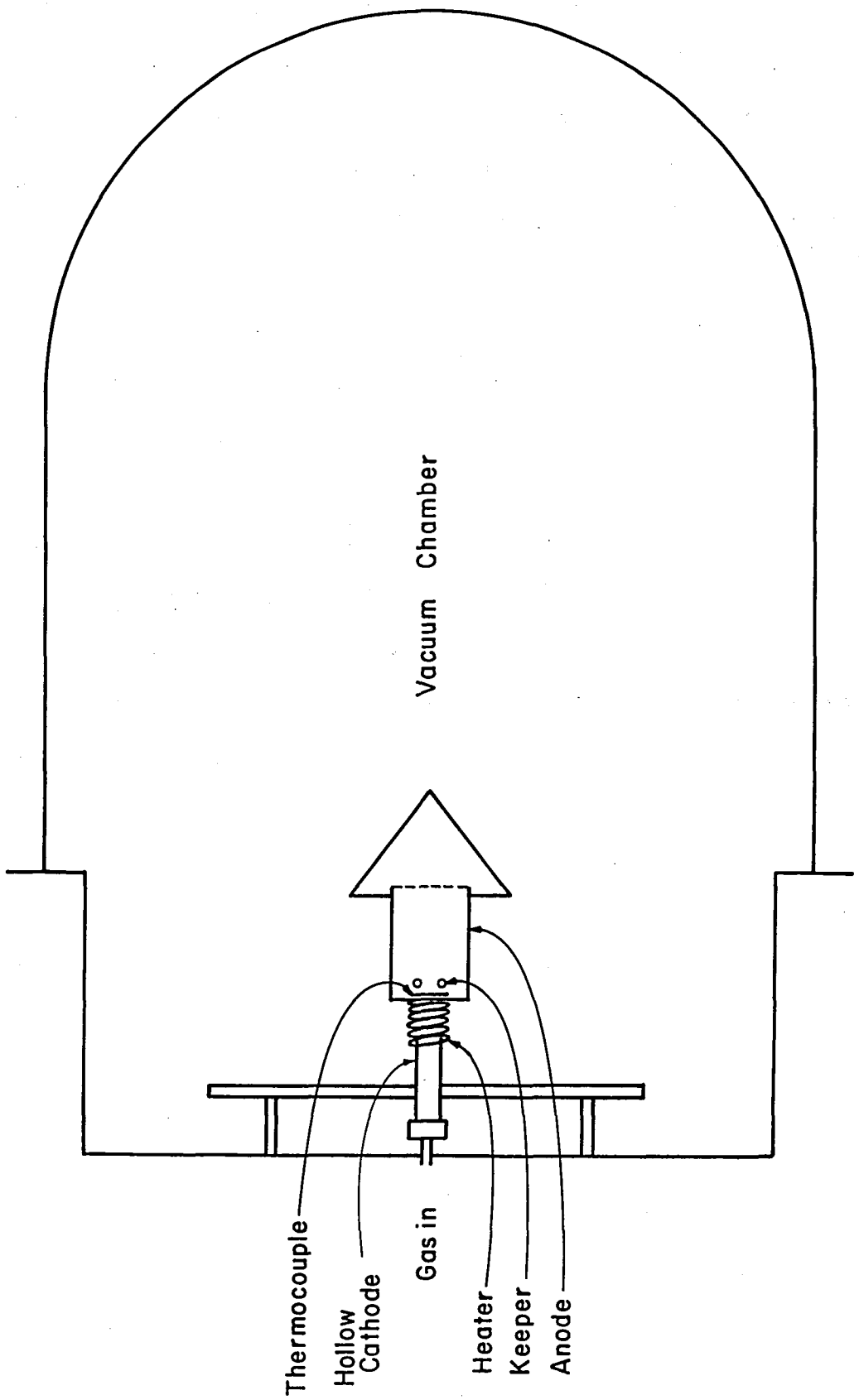

Fig. 2-1. Diagram of 45-cm vacuum chamber and hollow cathode plasma generating apparatus.

bell-jar size. With shorter lengths at low densities, the analysis procedure gives ambiguous results. At densities of 10^8 cm^{-3} a spherical probe of similar surface area (1.3 cm diameter) was tried and showed excellent correlation with the cylindrical probe. This spherical probe of 1.3 cm diameter provided reliable measurements down to the desired minimum bell jar densities of 10^5 cm^{-3}. A spherical probe of smaller diameter, 1 cm, was also tested and compared to the larger spherical probe at the same plasma conditions. Electron temperature, plasma density, and plasma potential were in good agreement, within less than 20% difference at 10^6 cm^{-3}.

The spherical probe was monitored before, during, and after experiments. In order to initially adjust the hollow cathode to provide a desired density, a rapid means of checking plasma density was needed. Because complete analysis of a Langmuir probe trace is too lengthy and time consuming to be performed during testing, a quick method was needed to correlate plasma density with a simple measurement.

An excellent correlation was found between (1) the slope of the current-voltage probe characteristic at a chosen reference point, and (2) the plasma density obtained from a complete analysis of the probe characteristic. The correlation is shown in Fig. 2-2.

The straight line is a least squares fit and can be expressed as

$$n = 1.96 \times 10^8 \, (\Delta I/\Delta V)^{0.99} \qquad (2\text{-}1)$$

or for laboratory application,

$$n \approx 1.96 \times 10^8 \, \Delta I/\Delta V \qquad (n \text{ in } cm^{-3}, \ \Delta I/\Delta V \text{ in mA/V}) \qquad (2\text{-}2)$$

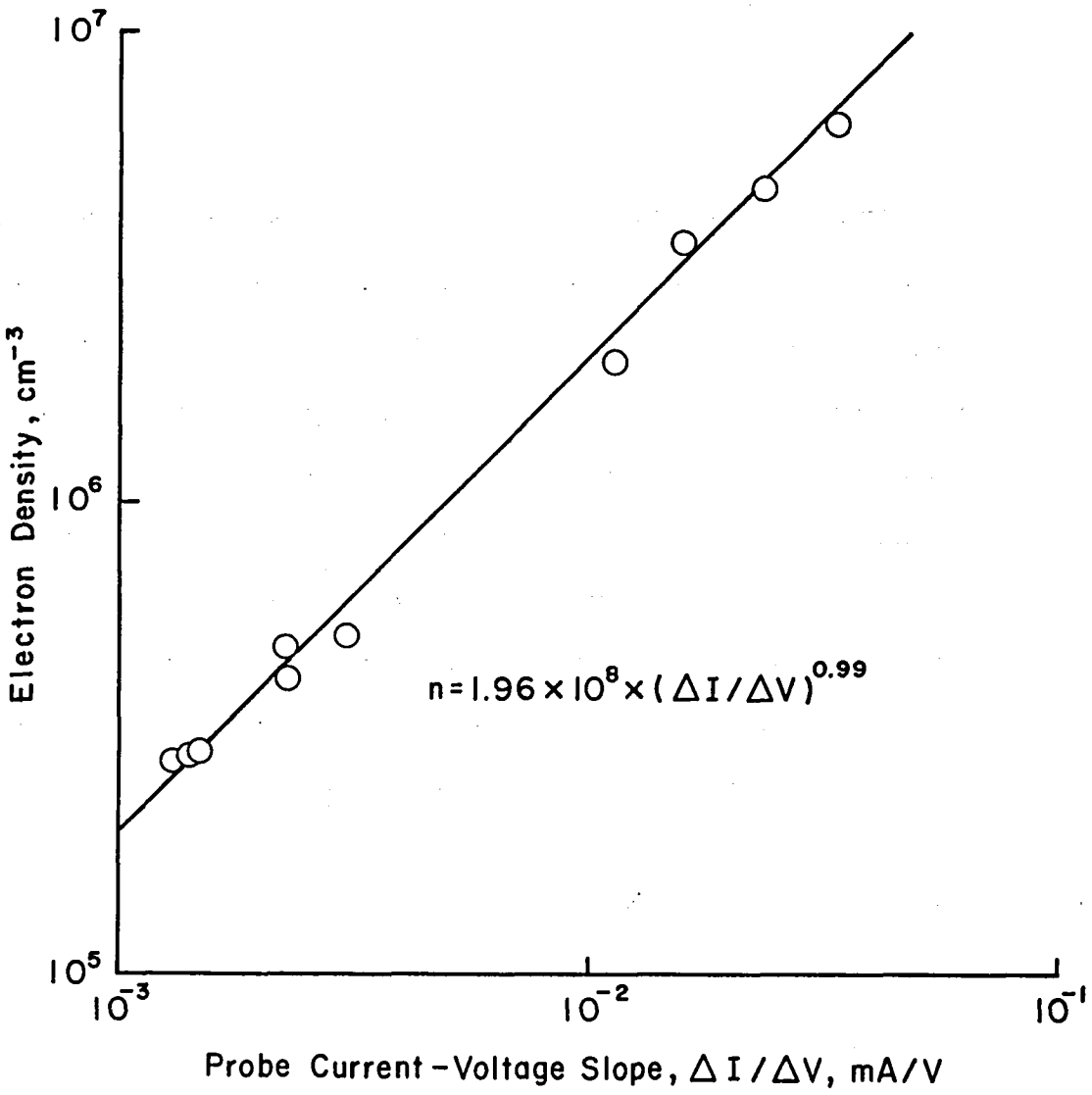

Fig. 2-2. Correlation between the slope of the Langmuir probe characteristic and the electron density.

To determine a satisfactory location for the sample in the bell jar, a plasma density survey was made. Six positions (shown in Fig. 2-3) were evaluated. Table 2.1 lists the survey locations and their corresponding plasma densities and electron temperatures. The sample holders were mounted at position A.

Solar Array Simulation

Simplified models of solar cells were constructed which could be connected to a variable high voltage power supply in series with a sensitive ammeter (see Fig. 2-4). The models were shielded from the plasma by overlaying sheets of insulating materials such as polyimide. Small holes drilled in the insulating material represented defects caused by manufacturing processes or micrometeorites. The solar cells themselves were represented by the underlying conductor. The simplest model (see Fig. 2-5) was made by etching a printed circuit board to leave a 7.9 cm copper disc centered on a 12 cm × 12 cm fiberglass backing. An electrical connector was soldered to the copper disc from the rear of the board to provide insulated connection to the high voltage power supply. The entire front surface of the sample board was then covered with a polyimide insulating sheet attached by adhesive, with the adhesive no closer than 5 mm to the hole and usually farther away. A later variation of this basic model permitted the copper disc to be rotated beneath the insulator to renew the exposed metal surface. This rotation permitted clean conductor to be exposed without any other changes.

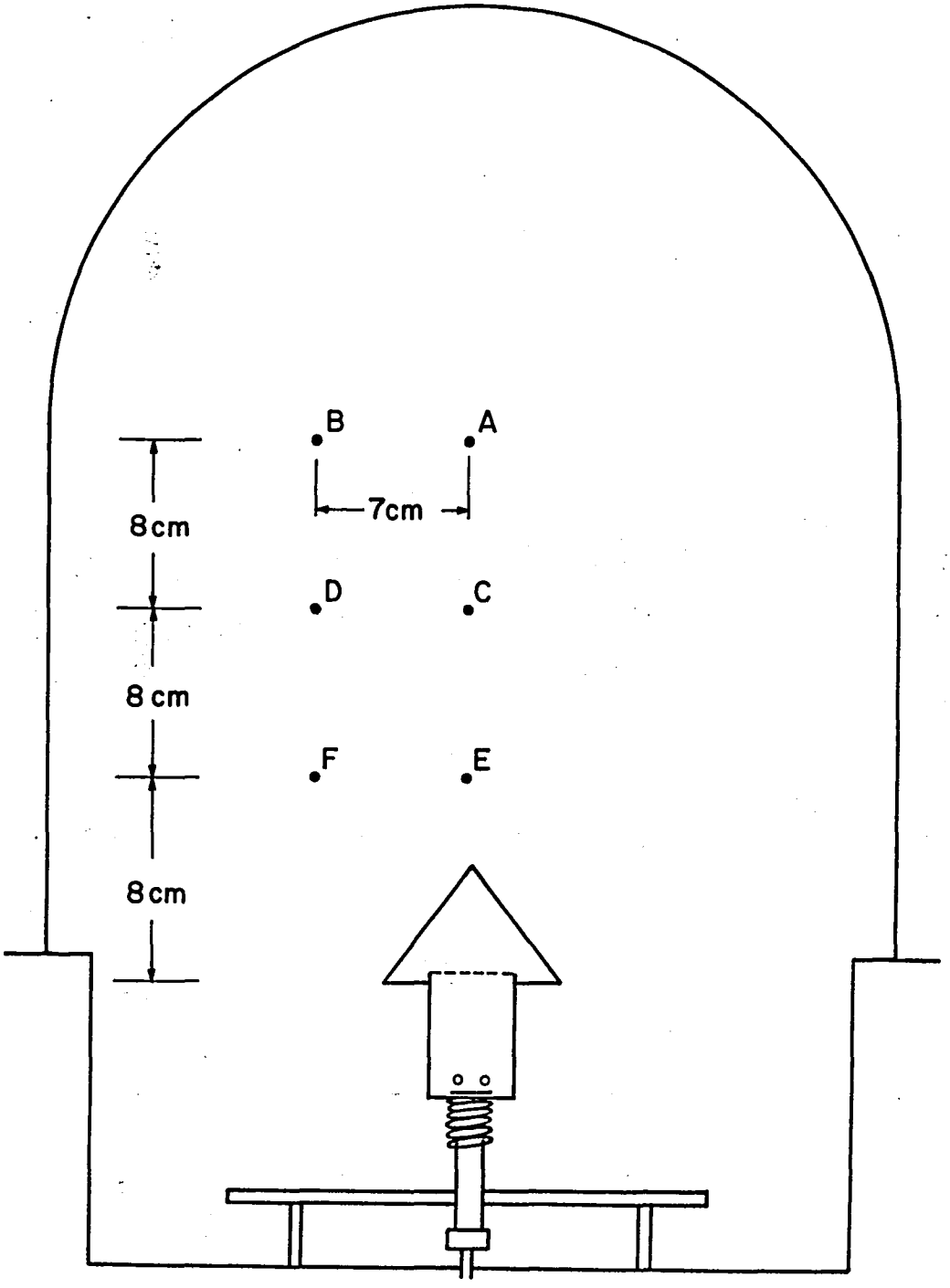

Fig. 2-3. Plasma survey locations in vacuum chamber.

Table 2-1. Electron Density and Temperature Profile

Position	Electron Density	Electron Temperature
A	4.79×10^5 cm^{-3}	2.03 eV
B	3.82×10^5 cm^{-3}	1.62 eV
C	3.25×10^5 cm^{-3}	2.32 eV
D	4.62×10^5 cm^{-3}	2.25 eV
E	1.33×10^6 cm^{-3}	3.24 eV
F	3.33×10^6 cm^{-3}	2.12 eV

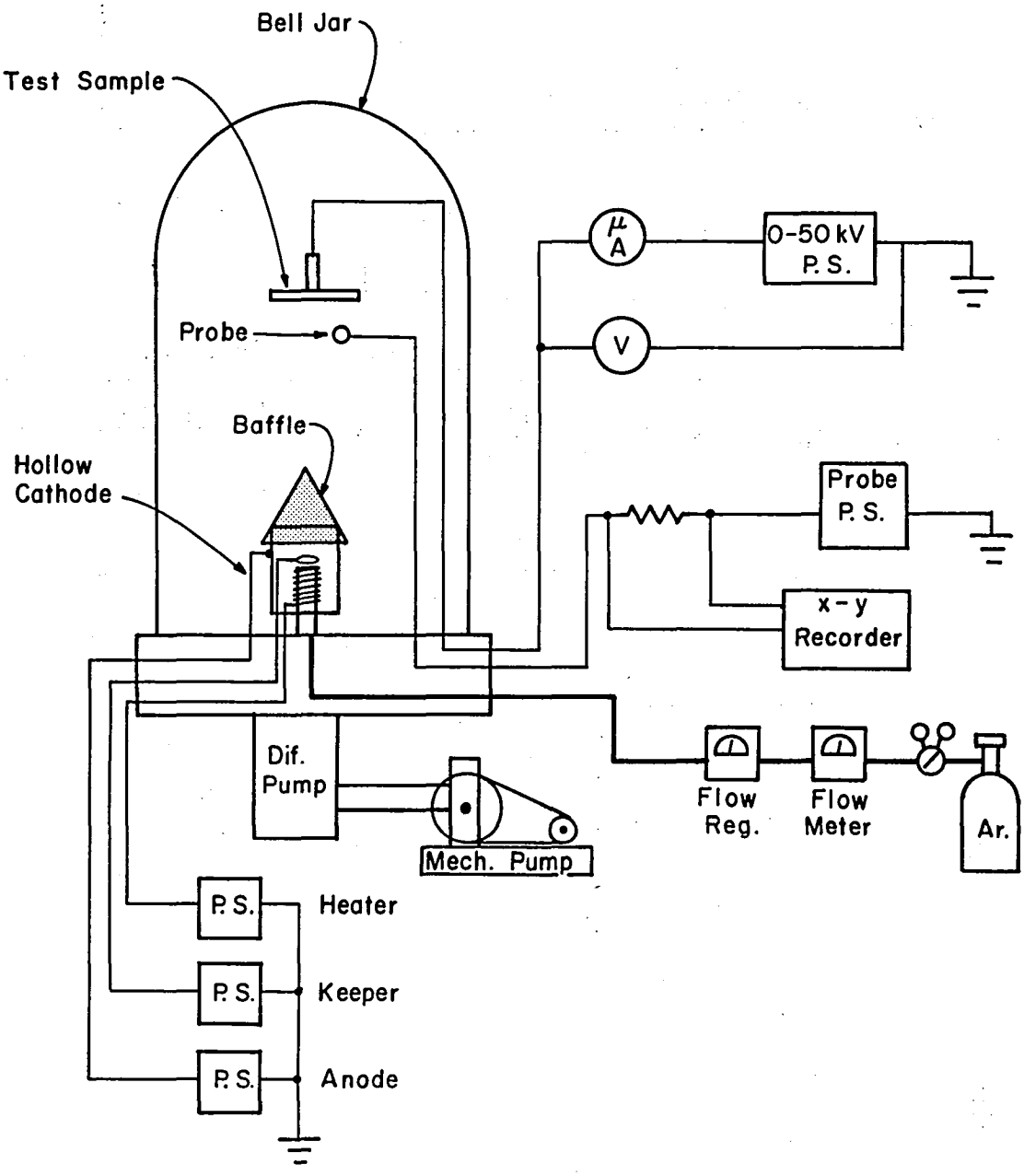

Fig. 2-4. Test set-up schematic.

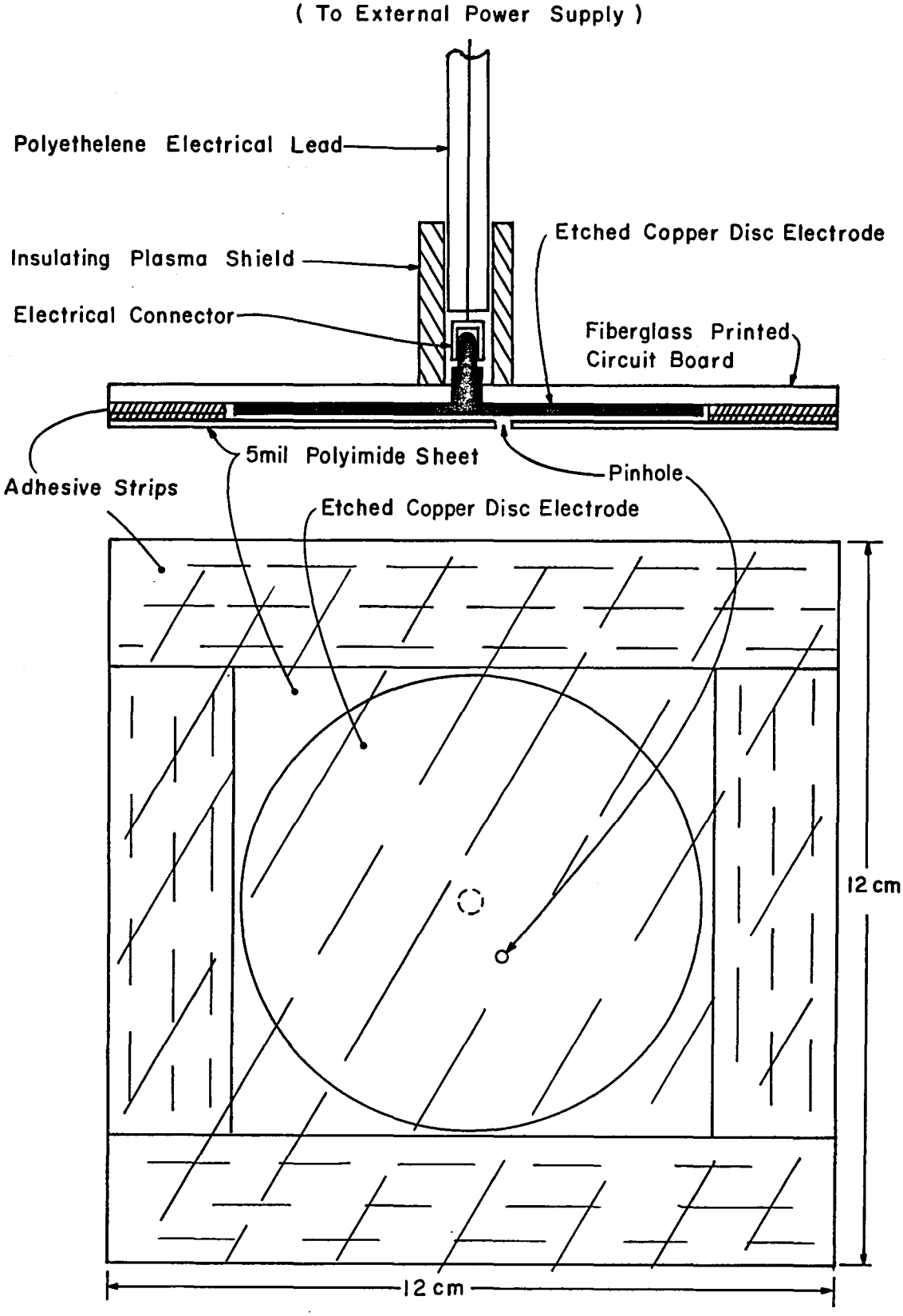

Fig. 2-5. Solar cell model.

Procedure

The solar cell models were centrally mounted in the evacuated bell jar and a plasma of the desired density was established by adjusting the argon hollow cathode while monitoring the density with the spherical Langmuir probe. A slowly increasing positive voltage was then applied to the metal disc of the sample causing current to be extracted from the plasma through the small hole drilled in the insulating sheet. The resulting current vs. voltage data were recorded. Langmuir probe traces were also made to confirm plasma conditions. Test variables included: insulating materials, insulating area, insulating surface configuration, and defect hole number.

III. EXPERIMENTAL RESULTS

Robert P. Stillwell
Donald C. Trock

Probe with Conducting Shield

In order to make a comparison between planar probe theory (see Appendix B) and current collected by a pinhole defect in a solar cell, a planar probe was constructed. As seen in Fig. 3-1, the planar probe consisted of a 1 mm diameter piece of stainless steel in a quartz tube of outside diameter 1.98 mm. A quartz tube was then sealed in a hole in a piece of printed circuit board 15.2 cm by 19.1 cm, with the printed circuit board covered with copper. The stainless steel rod was flush with the copper layer on the printed circuit board and connected to the high voltage lead.

Figures 3-2 and 3-3 are typical examples of the correlation between the planar probe theory and experimental results. The theory is presented in Appendix B, together with experimental data to justify the use of 1.8 for the adjustable parameter b in Eq. (B-4). Above several hundred volts, the data are within ± 50 percent of the theory. Compared to variations with an insulating shield, this ± 50 percent is in close agreement.

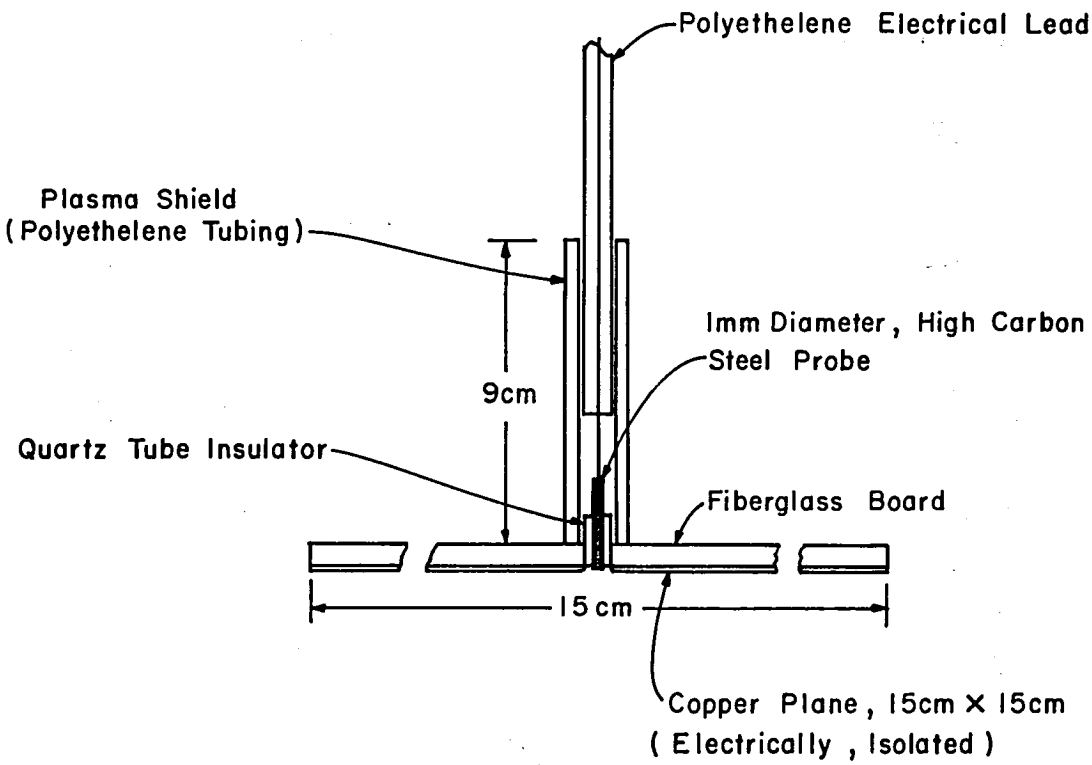

Fig. 3-1. Schematic representation of planar probe.

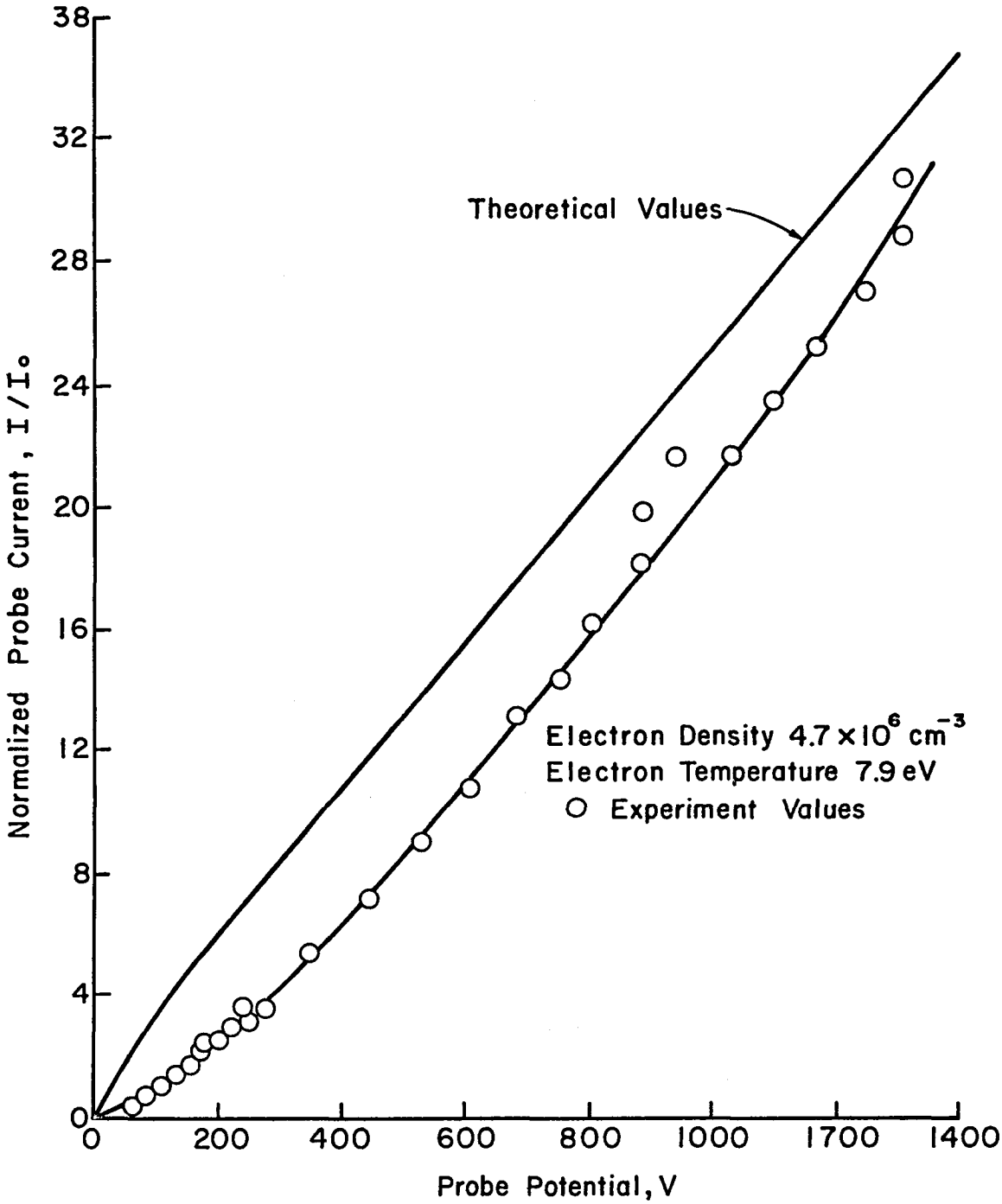

Fig. 3-2. Comparison between experimental and theoretical planar probe current for an electron density of 4.7×10^6 cm^{-3}.

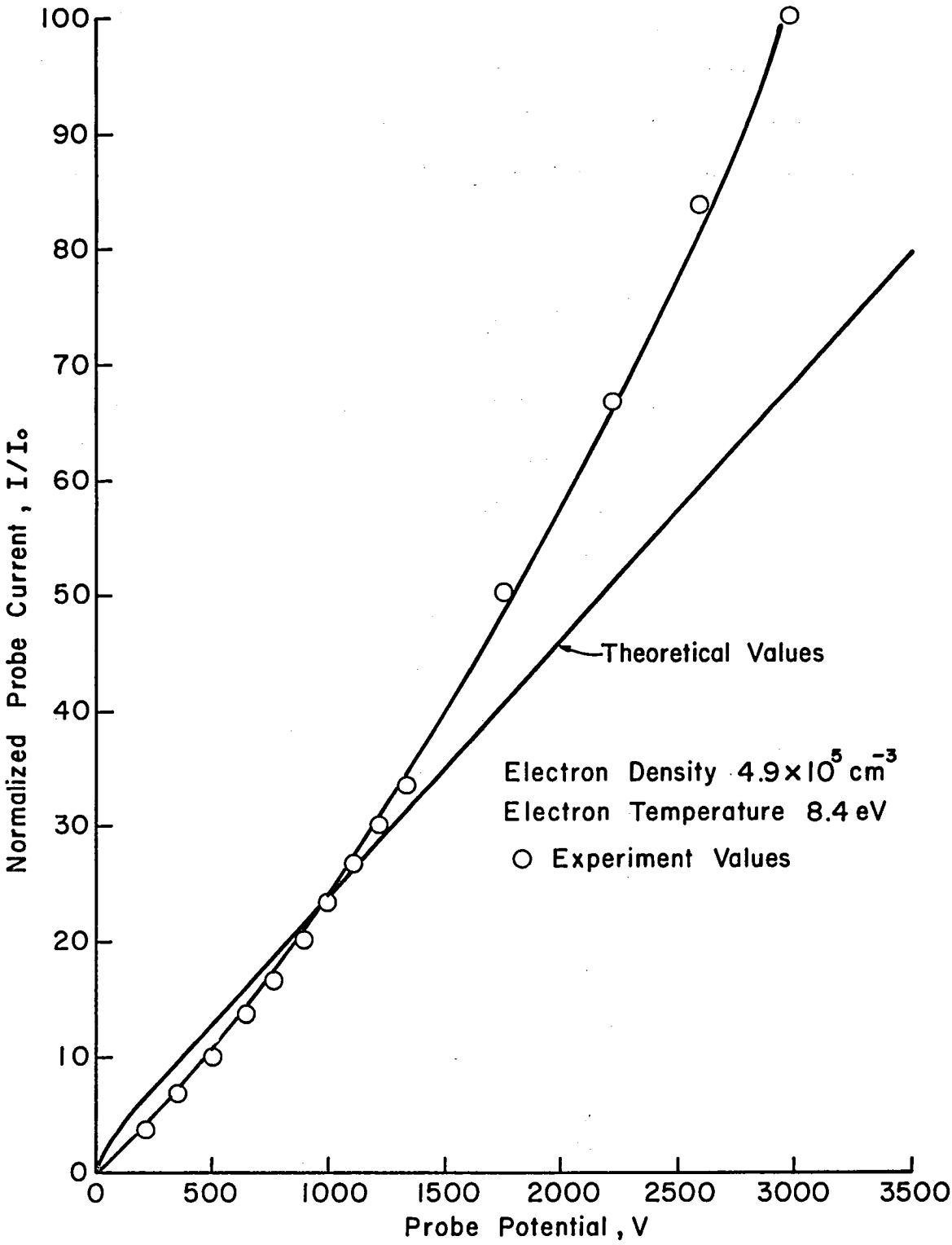

Fig. 3-3. Comparison between experimental and theoretical planar probe current for an electron density of 4.9×10^5 cm^{-3}.

Normalization

All currents reported herein are normalized for small variations of electron density, temperature and pinhole area. Collected currents are normalized by the factor I_o where

$$I_o = Aen\left(\frac{T_e}{2\pi m_e}\right)^{\frac{1}{2}} \tag{3-1}$$

and A is the area of conductor exposed by pinhole, e is the electronic charge, n is the electron density in the plasma, T_e is the electron temperature, and m_e is the electronic mass.

This current is simply the random electron flux[1] to the projected hole or conductor area in the plasma under consideration. Small variations in plasma properties between runs were typically observed, even with the use of the approximate relationship of Eq. (2-2) to set up test conditions. The use of a normalized current therefore resulted in less variation between runs and clearer experimental trends. Note that the currents of Figs. 3-2 and 3-3 were presented in normalized form.

Evaluation of Simulated Solar Cell Insulated with Plain Polyimide

The objective of this series of tests was to determine the current-voltage characteristics of a simulated solar cell insulated with a plain piece of polyimide with a defect in the insulation. The defect in the insulator consisted of a 1 mm diameter pinhole drilled into a piece of polyimide. The polyimide was then placed on a simulated solar cell with an adhesive. These samples were then placed in a bell jar,

and the current-voltage characteristics recorded. As mentioned previously, the adhesive was 5 mm, or more, from the hole.

Figure 3-4 compares the current predicted by planar probe theory with typical currents observed. Note that the observed currents differ from theoretical values by up to 3 orders of magnitude. This confirms the results of previous investigations that found electron currents far in excess of what would be expected from electrostatic theory.

Figure 3-5 shows a typical current-voltage characteristic of a plain polyimide sample on linear scales (same data as Fig. 3-4). For similar samples, the normalized values of current were found to be consistent within an order of magnitude in the extreme and typically agreed within a factor of 2 (see Fig. 3-6).

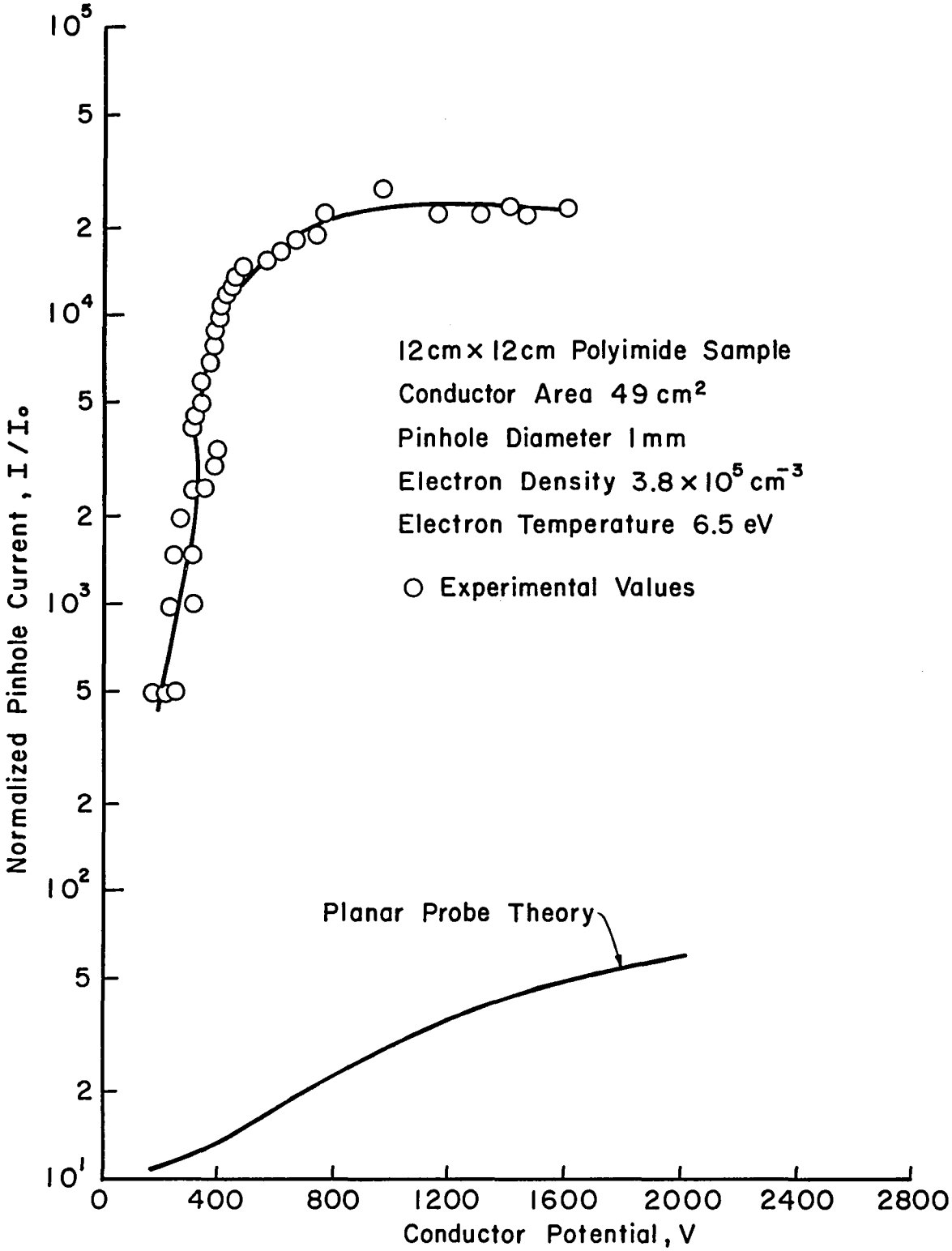

Fig. 3-4. Comparison of current collected by pinhole in a 12 cm × 12 cm piece of polyimide with current predicted by planar probe theory.

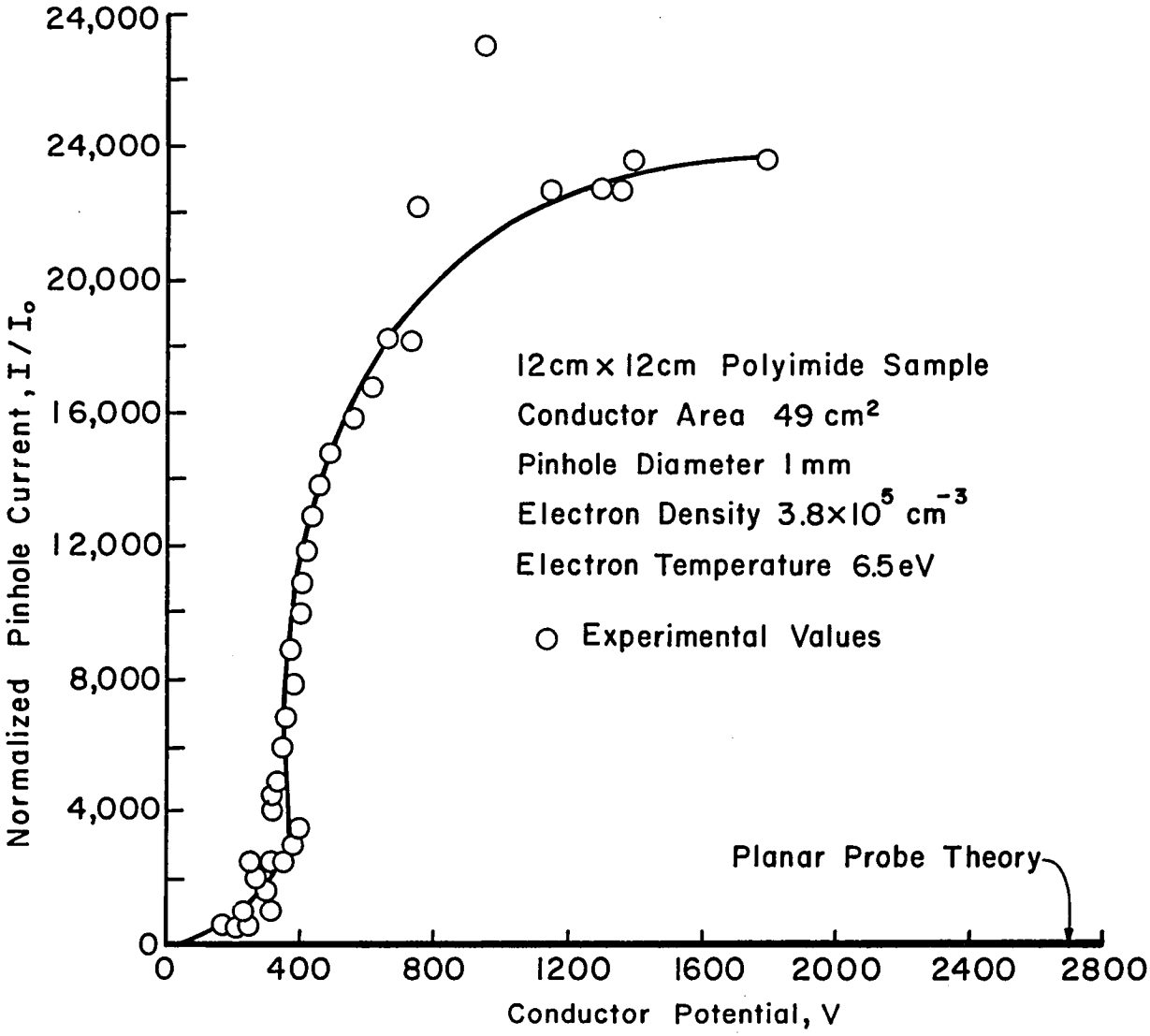

Fig. 3-5. Comparison of current collected by pinhole by a 12 cm × 12 cm piece of polyimide with current predicted by planar probe theory.

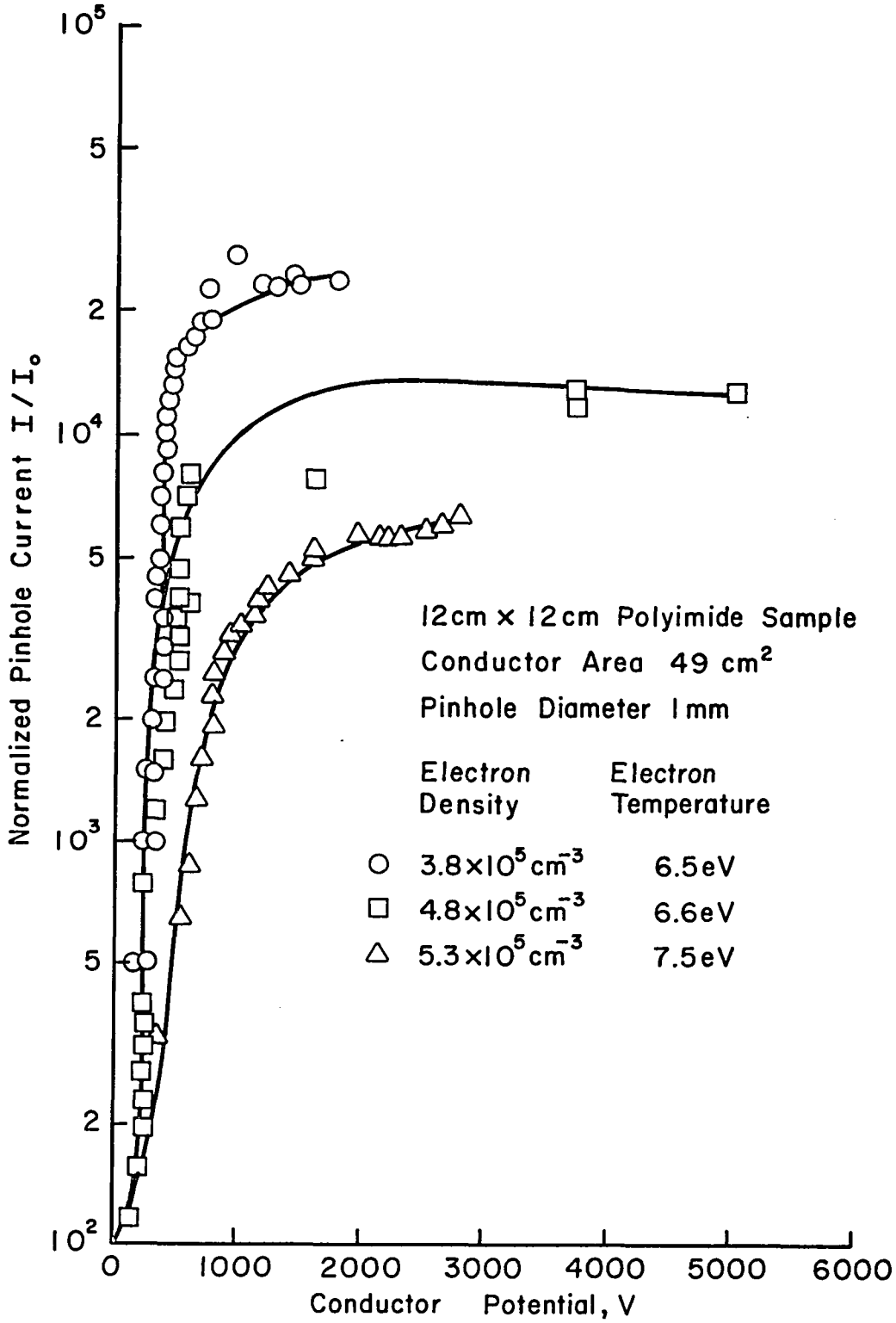

Fig. 3-6. Comparison of three 12 cm × 12 cm polyimide samples to show extremes in data.

Fresh and Old Samples

Subsequent tests made on the same sample showed a variation of the data. Figures 3-7 and 3-8 show some typical curves for both initial and subsequent tests. Two trends are indicated in Figs. 3-7 and 3-8. The general degradation in current conduction with repeated tests shown in Fig. 3-7 is the typical trend. The apparent restoration of high currents by simply waiting was not typical, but serves to indicate some of that data variation that was encountered. Subsequent tests with delays between tests did not show similar effects.

After a test with a "fresh" hole (i.e., a newly drilled hole that had not yet had current conducted through it), the hole was inspected. It was found that the pinhole appeared slightly melted and that a small deposit of some vitreous or shiny material was visible on the inner rim of the pinhole. Resistance tests were attempted and the deposited material could not be shown to be conductive. After a test, a fresh hole always showed the changes cited, but these holes could be made to perform the same as fresh holes by merely mechanically scraping smooth the interior of the hole with a drill of the appropriate size and not altering the upper surface of the Kapton. That is, the saturation current again returned to its former high values sometimes increasing by as much as an order of magnitude merely as a result of mechanically scraping the interior rim of the hole. The holes were used in as many as four tests (Fig. 3-9) with the performance restored to near original values by reaming out the hole.

Four possible models were put forth in an attempt to understand the effect of repeated tests. The first is that the "old-hole fresh-hole"

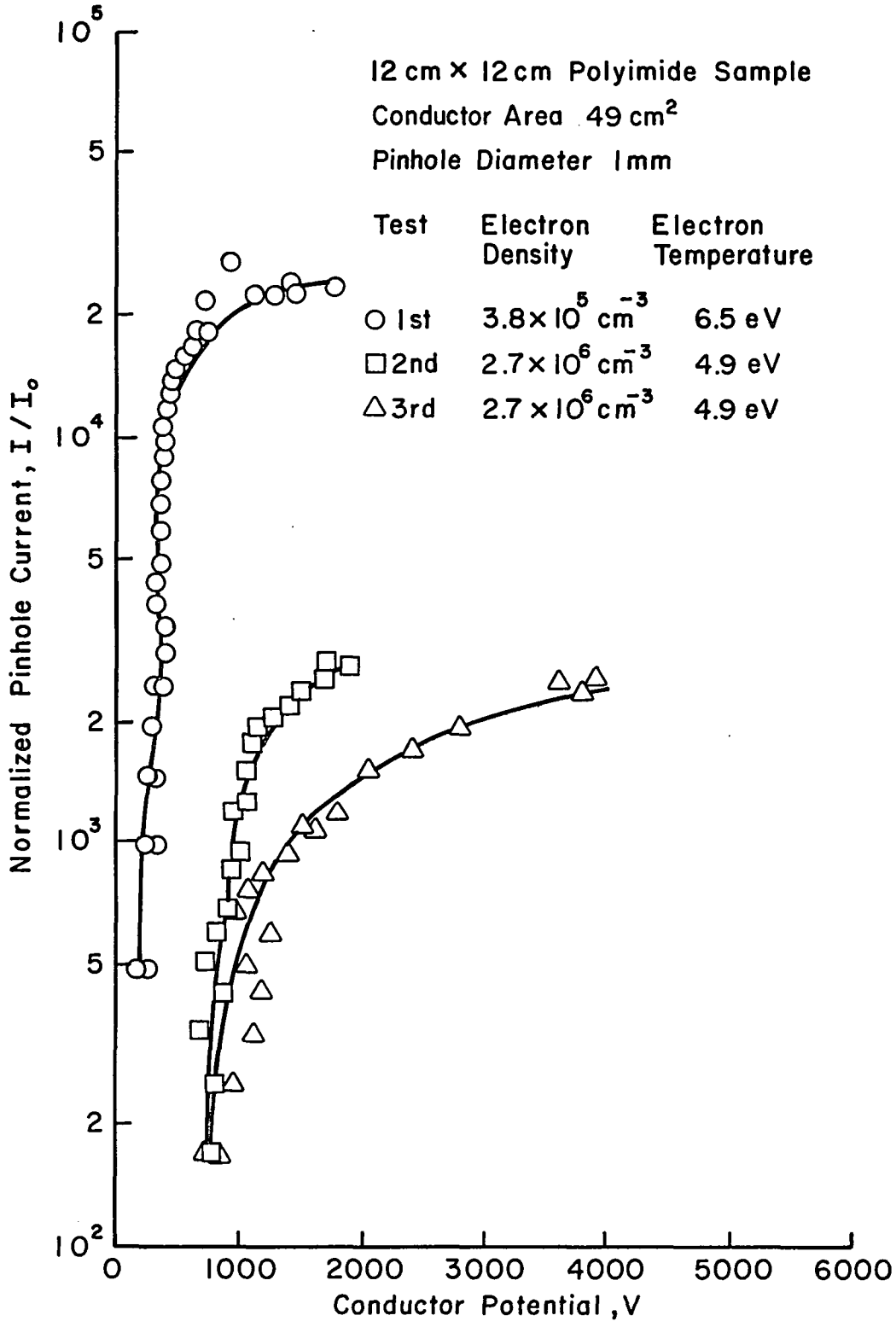

Fig. 3-7. Comparison between the first, second and third tests of a 12 cm × 12 cm polyimide sample.

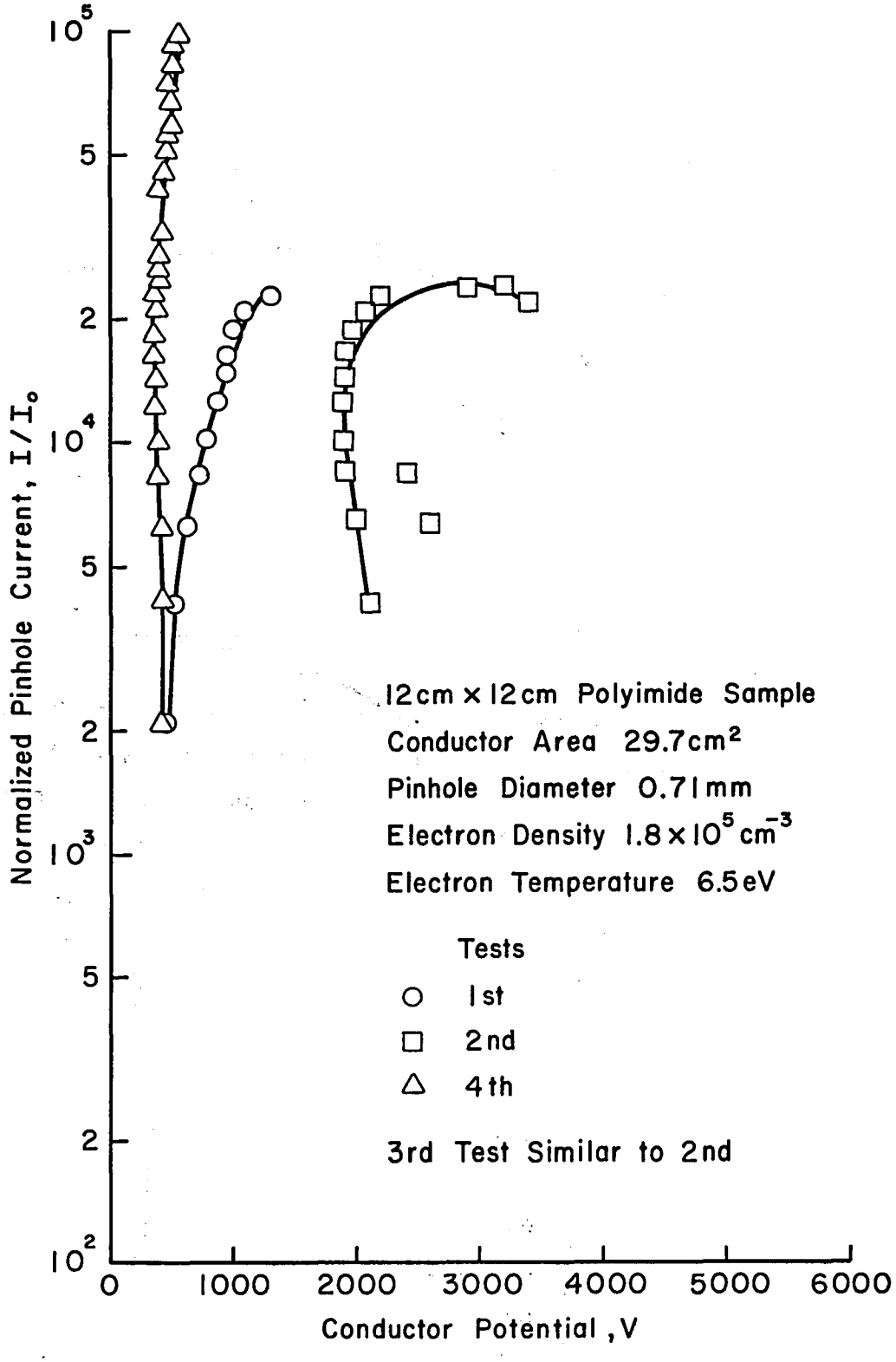

Fig. 3-8. The first, second and fourth tests of a 12 cm × 12 cm polyimide sample.

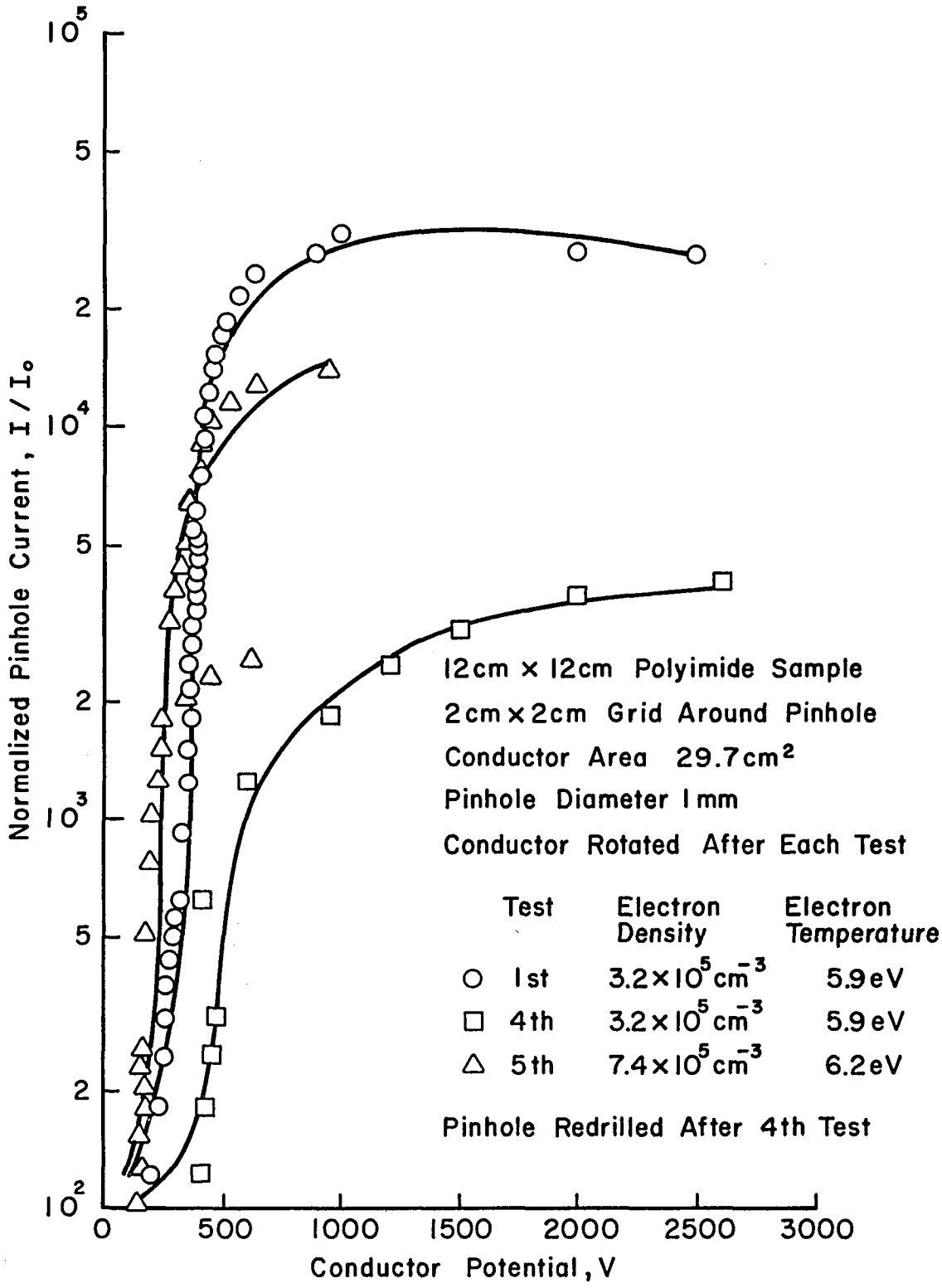

Fig. 3-9. Comparison of tests before and after pinhole has been redrilled.

effect is due to absorbed gas layers on the polyimide. As time passes, the plasma removes the absorbed layers by bombardment, decreasing the amount of gas released, and thereby decreasing both the plasma density near the hole and the current collected. This model was tested by using a fresh sample, then removing the sample from the bell jar and exposing it to air (for 17 hours), then replacing the sample and testing it again. Figure 3-10 shows the results of these tests. It appears unlikely that adsorbed gases are the cause of this "old-hole fresh-hole" effect.

A second model examined was that the polyimide is being vaporized, and that this vapor around the pinhole becomes conductive through ionization. After a time, the available material in the pinhole (either a volatile component or surface irregularities that are easily heated and vaporized) might be depleted, resulting in a decrease in vapor pressure around the pinhole, thus decreasing the current collected through the pinhole. A glass sample was constructed to further test this model and will be discussed in a later section.

The third possibility is that in the manufacturing process, the molecules are stretched out in long polymer chains, which, while electrically insulating normal to the polyimide surface might possibly be a poor conductor along the surface. When the polyimide is heated, these polymer chains might be broken, disrupting the conduction. By scraping the interior of the old hole, fresh Kapton would be exposed, leaving fresh volatile material or exposing fresh polymer chains.

This third possibility was tested by placing a strip of polyimide 3 cm × 10 cm in the bell jar and applying 5000 volts, end to end. No detectable current could be measured. A neutral argon background was

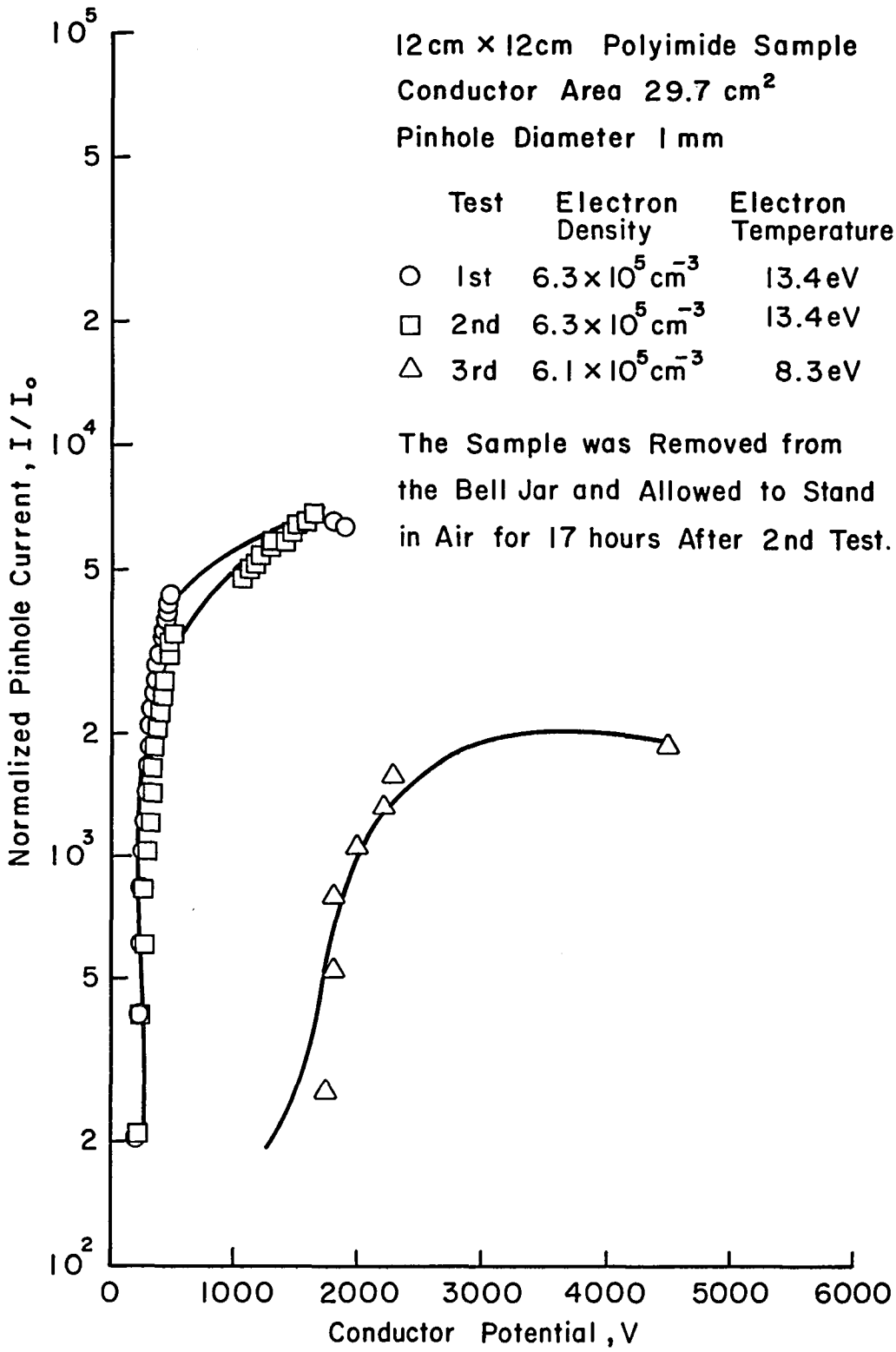

Fig. 3-10. Comparison of first, second and third tests showing "old-hole fresh-hole" effect unchanged by exposure to air.

then added, and still no current could be detected. This test was done for two different orientations of polyimide (see Fig. 3-11). These tests appeared to eliminate the third possibility of conducting polymer chains.

The fourth possible model is that the polyimide is being vaporized by the heat generated in the area where visible light emission is observed, then when the voltage is turned off, the vaporized polyimide condensed onto the conducting copper under the pinhole, producing an insulating barrier to subsequent current collection. To test this possibility, a conducting circle was constructed to be able to rotate under the polyimide, then after a test, the conductor could be rotated to a clean spot of copper. This was done but the saturation current still decreased with progressive tests. It can be concluded that an insulating coating on the copper did not cause this phenomenon.

As indicated above, only the second model was considered following the tests described. The generation of vapor from the insulator appears to be a material dependent process, as is the old-hole fresh-hole effect. Further discussion of vapor generation will be included with the discussion of other materials.

Effect of Insulator Area

As mentioned in Section I, an insulator area effect had been found in an earlier investigation. It therefore appeared appropriate to look for a similar effect in this investigation. To test for an area effect, three samples were constructed (see Table 3.1). The insulator areas in these three samples covered a 36:1 area range. All samples were

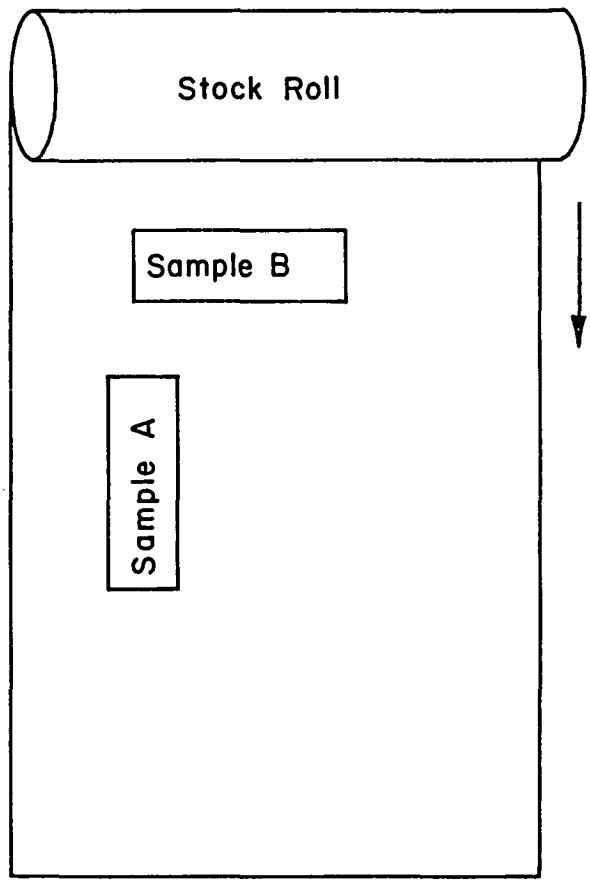

Fig. 3-11. Sketch of the two orientations of polyimide.

Table 3.1. Specifications of Area Test Samples

Sample	Polyimide Surface Area	Diameter of Pinhole	Diameter of Copper Circle Under the Polyimide
2 × 2	4 cm^2	1 mm	1.5 cm
5 × 5	25 cm^2	1 mm	4 cm
12 × 12	144 cm^2	1 mm	7.9 cm

constructed similar to sketch of Fig. 2-5 except that the dimensions of the two smaller samples were decreased from those of Fig. 2-5. These samples were tested and some typical results are shown in Fig. 3-12.

The conclusion drawn from Fig. 3-12 is that there is no appreciable difference in the current collected by different size samples. Thus the current collected by the pinhole does not seem to be a function of the area surrounding the pinhole for the plasma conditions studied and for the sample construction and sizes used. The constancy of the current at high voltages in Fig. 3-12 may indicate some saturation of the current from the available plasma. Some of the possible area effect may therefore be masked by this saturation.

Evaluation of Conductive Patterns on Polyimide Insulation

The objective of this series of tests was to examine the effect of conductive patterns on the polyimide insulation surrounding the pinhole defect. To provide the conductive pattern, copper tape with an adhesive backing was placed on the surface of the polyimide. Three patterns were used; copper tape 1.2 cm wide was placed around the rim of the back of the simulated solar cell, a 2 × 2 cm square was placed around the

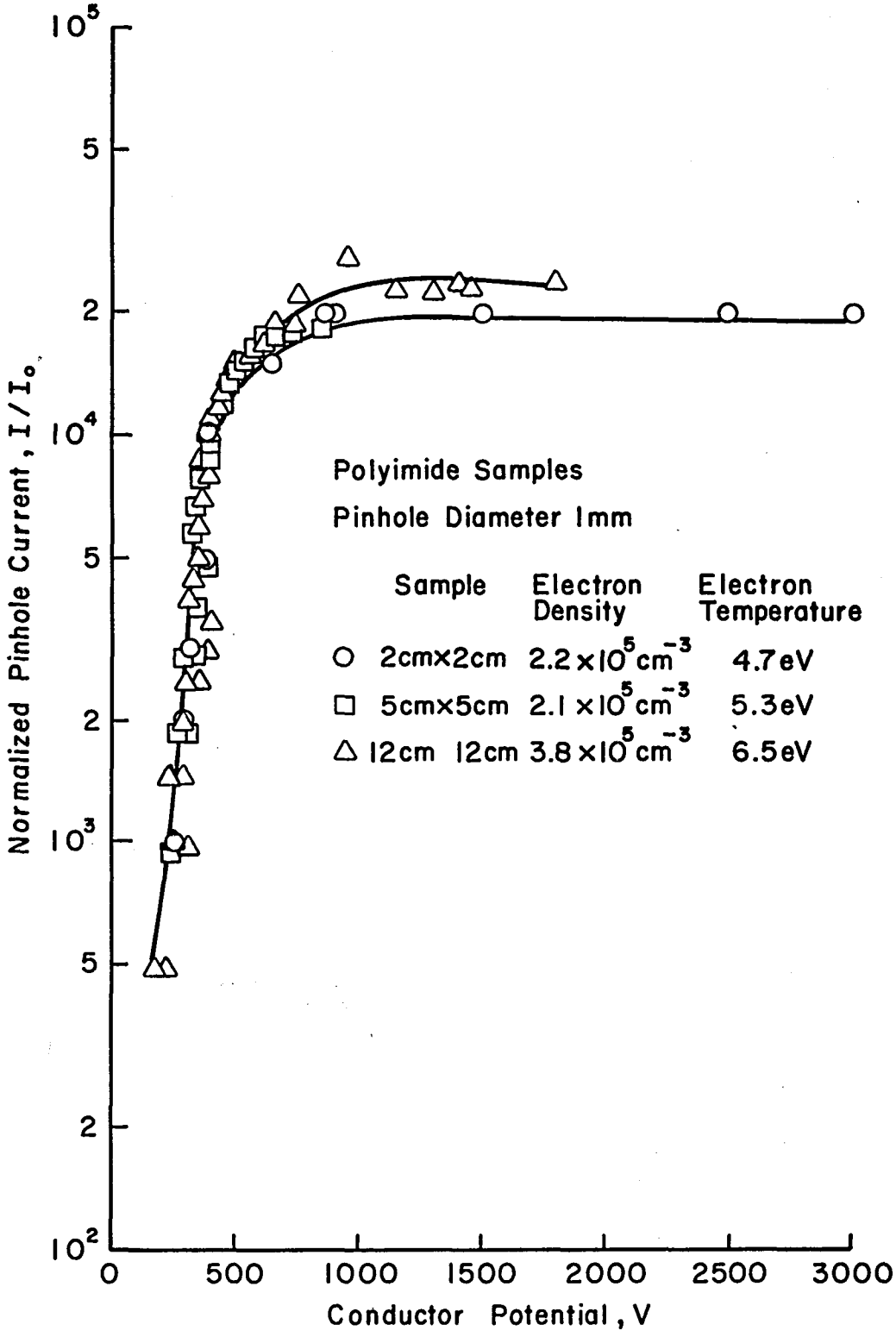

Fig. 3-12. Comparison of polyimide samples with different surface areas.

pinhole using 1.5 mm wide copper tape, and a grid was constructed of 1.5 mm wide copper strips placed 2 cm apart in such a way that there was a 2 × 2 cm square of unobstructed polyimide around the pinhole.

Conductive Rim on Back of Simulated Solar Cell. The effect of copper tape on the rim of the back (opposite to the hole) is shown in Figs. 3-13 and 3-14. Comparing in each case with a plain sample, the presence of the copper rim appeared to give a reduction in current collected. The reduction was within the typical factor of two scatter between tests, so this conclusion is not rigorous.

Conductive Square Surrounding Pinhole. The effect of a conducting square placed around the pinhole is shown in Fig. 3-15. In this graph there is no significant difference between the plain sample and one with the conducting square on it.

Conductive Grid on Polyimide Insulation. Placing a conductive grid on the insulator surface had a more noticeable effect on the current-voltage characteristic of the pinhole. As seen in Figs. 3-16 and 3-17, the level of current reached was reduced from that of the plain polyimide samples by a factor of 4 or 5 for both the 12 × 12 cm and 5 × 5 cm samples.

From these three conductor configurations is drawn the conclusion that conductors on the back of the sample are probably not significant. Small conductor areas on the front are probably also not significant, but a conducting grid over the entire front surface appears to give some reduction in current collection. This latter reduction is large enough that it exceeds the typical data variation, and is therefore probably significant.

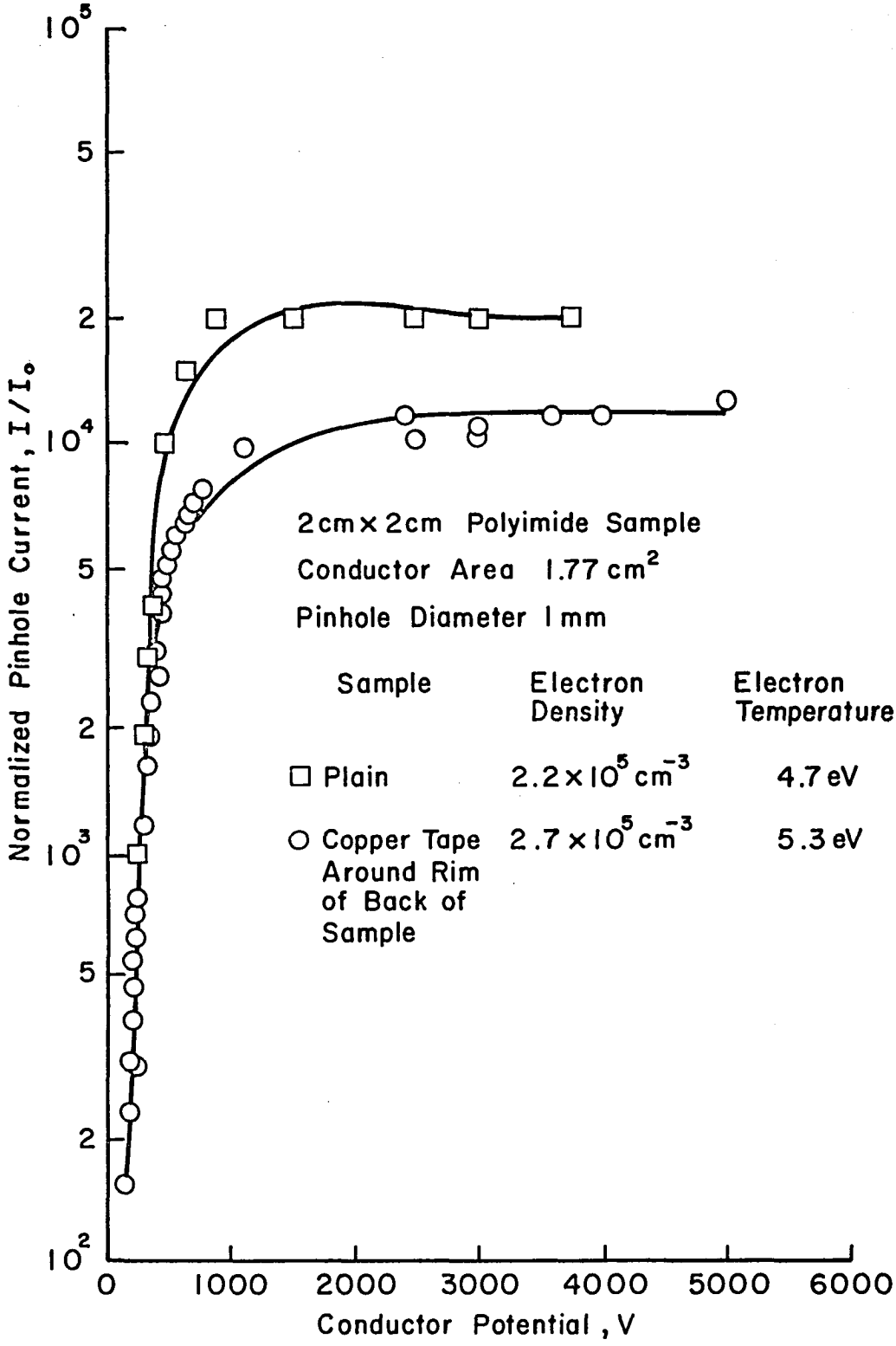

Fig. 3-13. Comparison of 12 cm × 12 cm polyimide samples with and without copper tape on rim of back of sample.

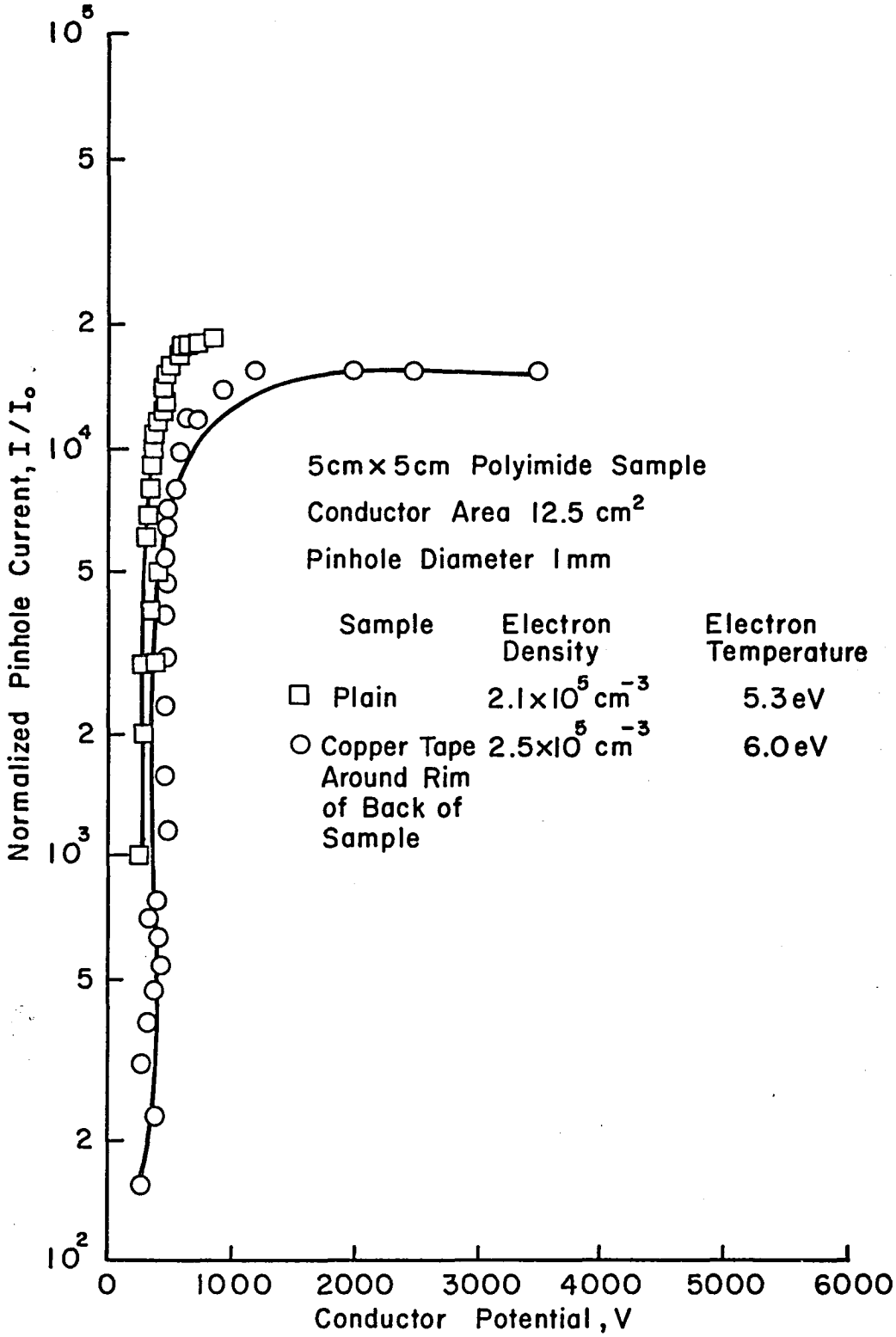

Fig. 3-14. Comparison of 5 cm × 5 cm polyimide samples with and without copper tape on rim of back of sample.

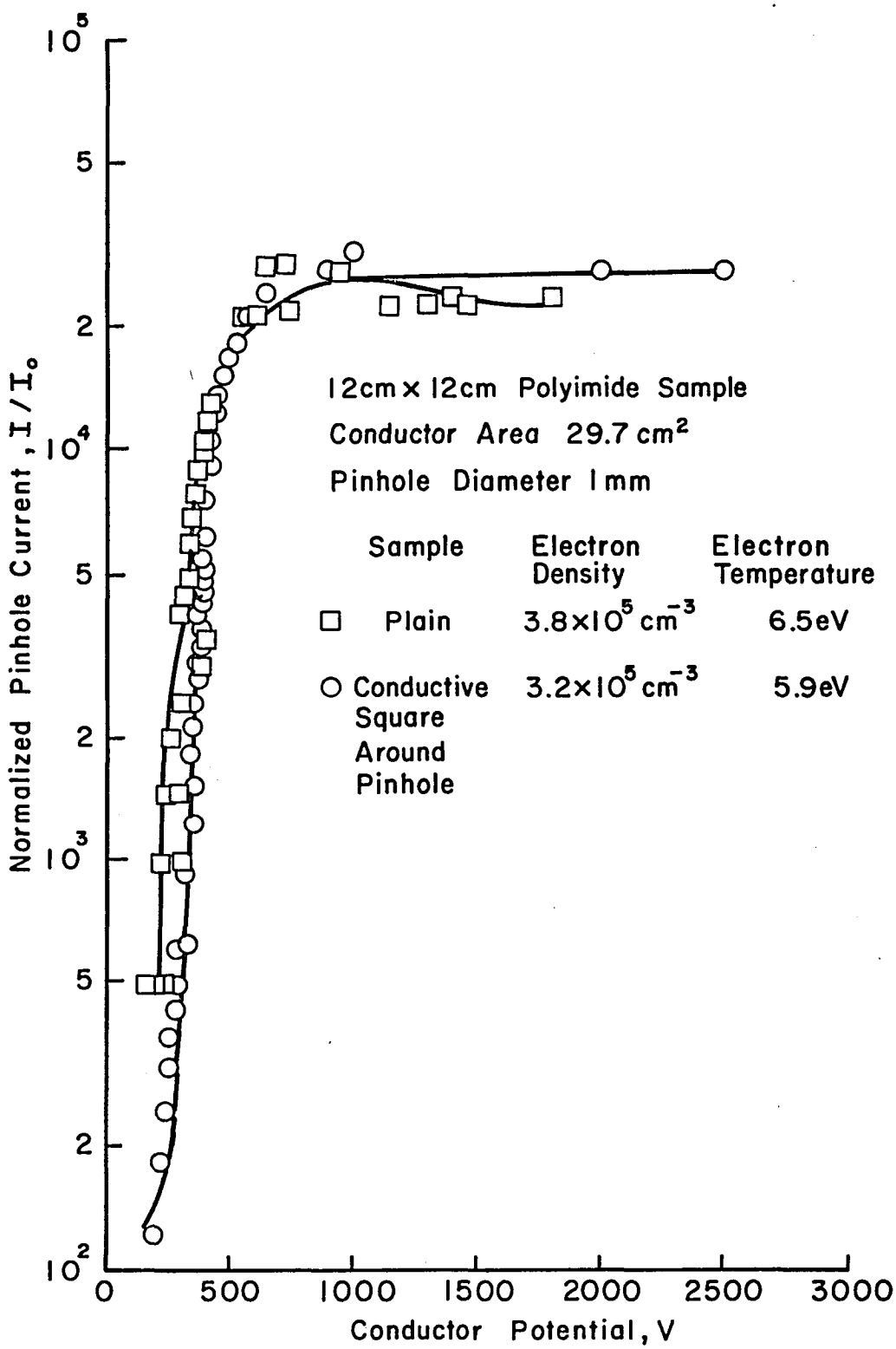

Fig. 3-15. Comparison between a polyimide sample with and without a 2 cm × 2 cm conductive square around pinhole.

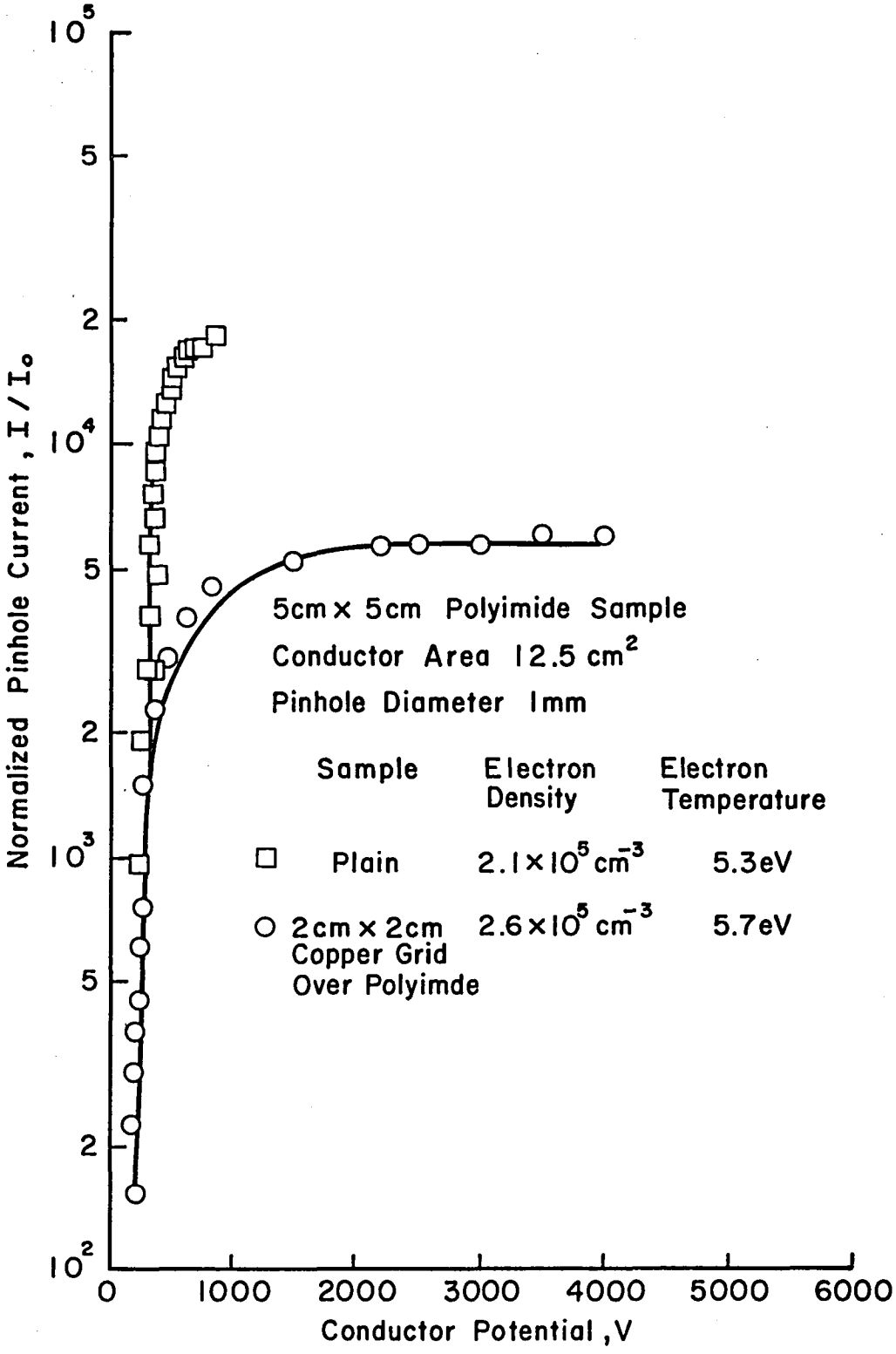

Fig. 3-16. Comparison between 5 cm × 5 cm polyimide sample with and without 2 cm × 2 cm copper grid over polyimide surface.

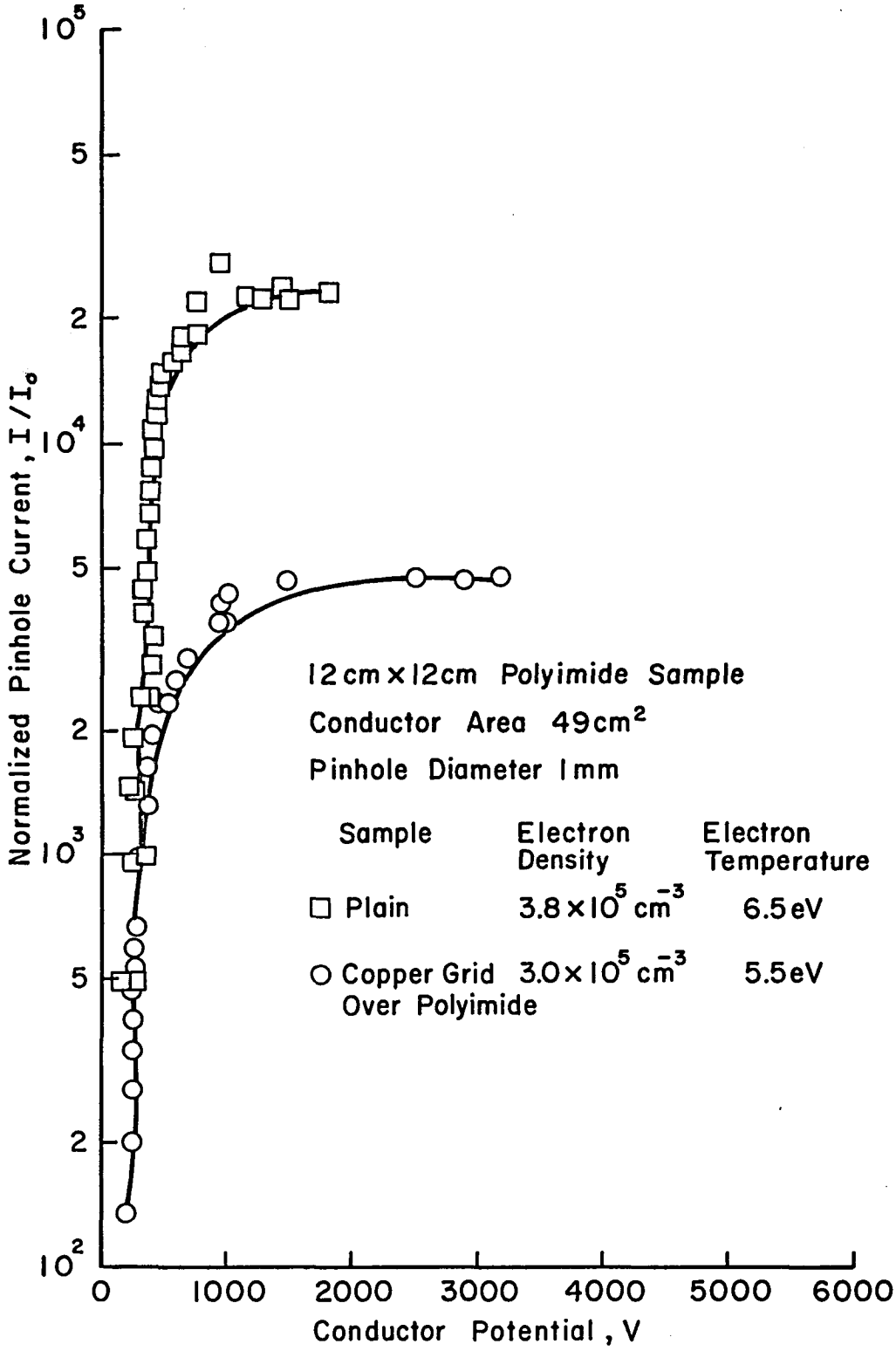

Fig. 3-17. Comparison between 12 cm × 12 cm polyimide samples with and without a copper grid over the polyimide surface.

Evaluation of Scribed and Ion Textured Patterns on Polyimide Insulation

The purpose of this series of tests was to determine if physical texturing of the surface of the polyimide insulation has an effect on the pinhole collection of current. These tests also provided additional data to evaluate possible surface effects in the current collection.

To texture the surfaces, a sharp metal stylus was used. The three patterns used were: a series of orthogonal lines scribed into the surface, Fig. 3-18(a); a series of concentric circles scribed into the surface, with the pinhole at the center, Fig. 3-18(b); and a series of radial lines originating from the vicinity of the pinhole, Fig. 3-18(c).

Figure 3-19 shows a comparison of the textured surfaces with a typical plain sample. It can be seen from the data that there is a consistent lowering of the current levels reached due to the texturing of the surfaces. Both the consistency of the results and the amount of the reduction indicate the observed effect is significant.

An attempt was also made to ion texture a polyimide surface, but no detectable texturing could be seen under an SEM (Scanning Electron Microscope).

Alternate Insulating Materials

The objective of this series of tests was to determine the effect of using different materials as insulators on the current-voltage characteristics of the pinhole. Three materials were used for these tests, mica, a silicon wafer, and glass.

Glass. As stated earlier, one possible model for the enhanced conduction was a vapor formed from the polyimide about the pinhole.

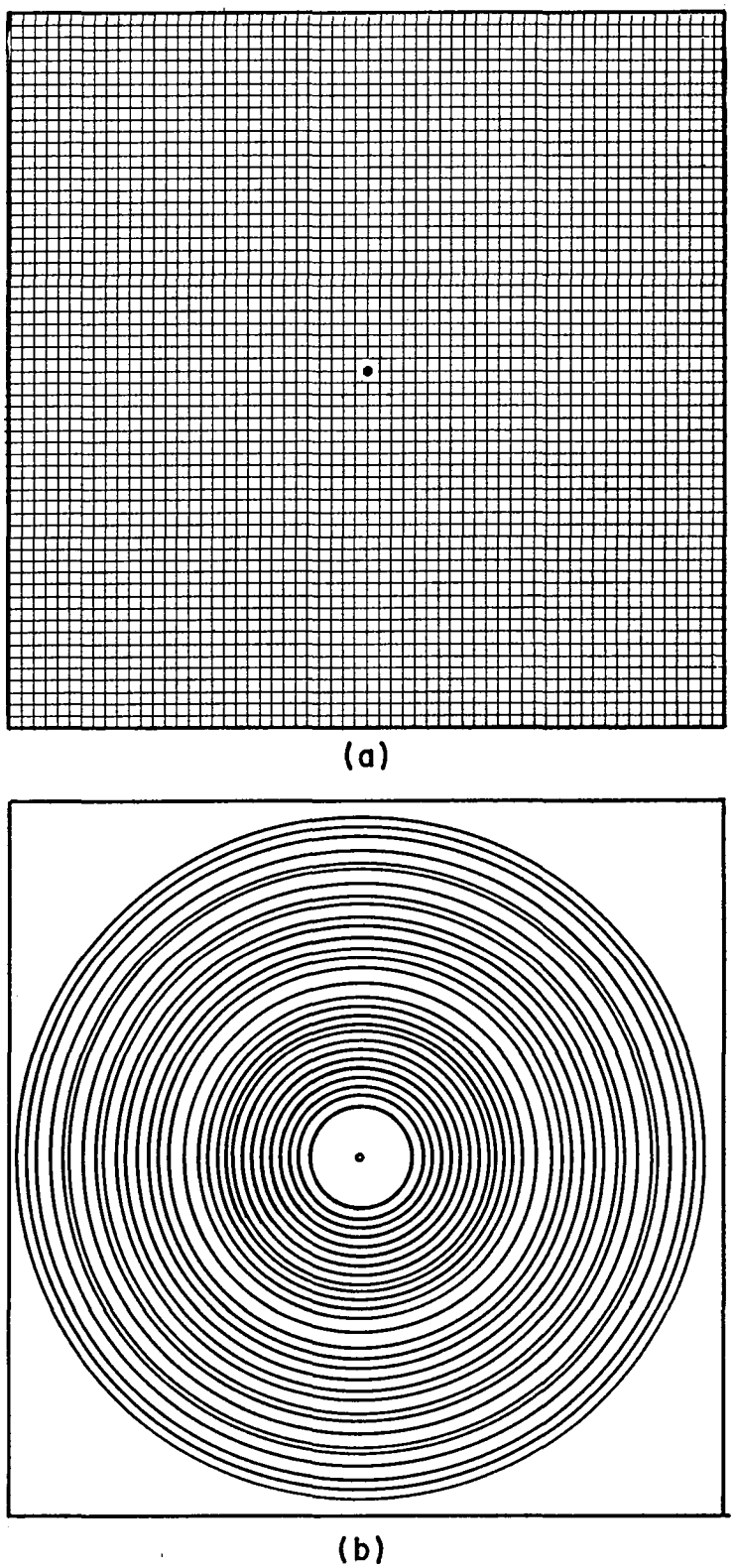

Fig. 3-18. Sketches of textured polyimide surfaces.

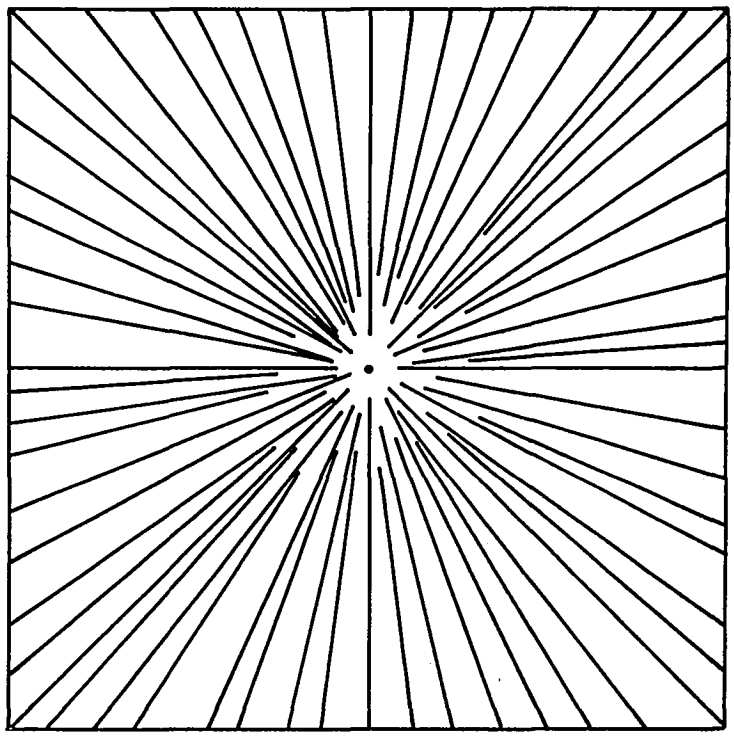

(c)

Fig. 3-18. (Continued)

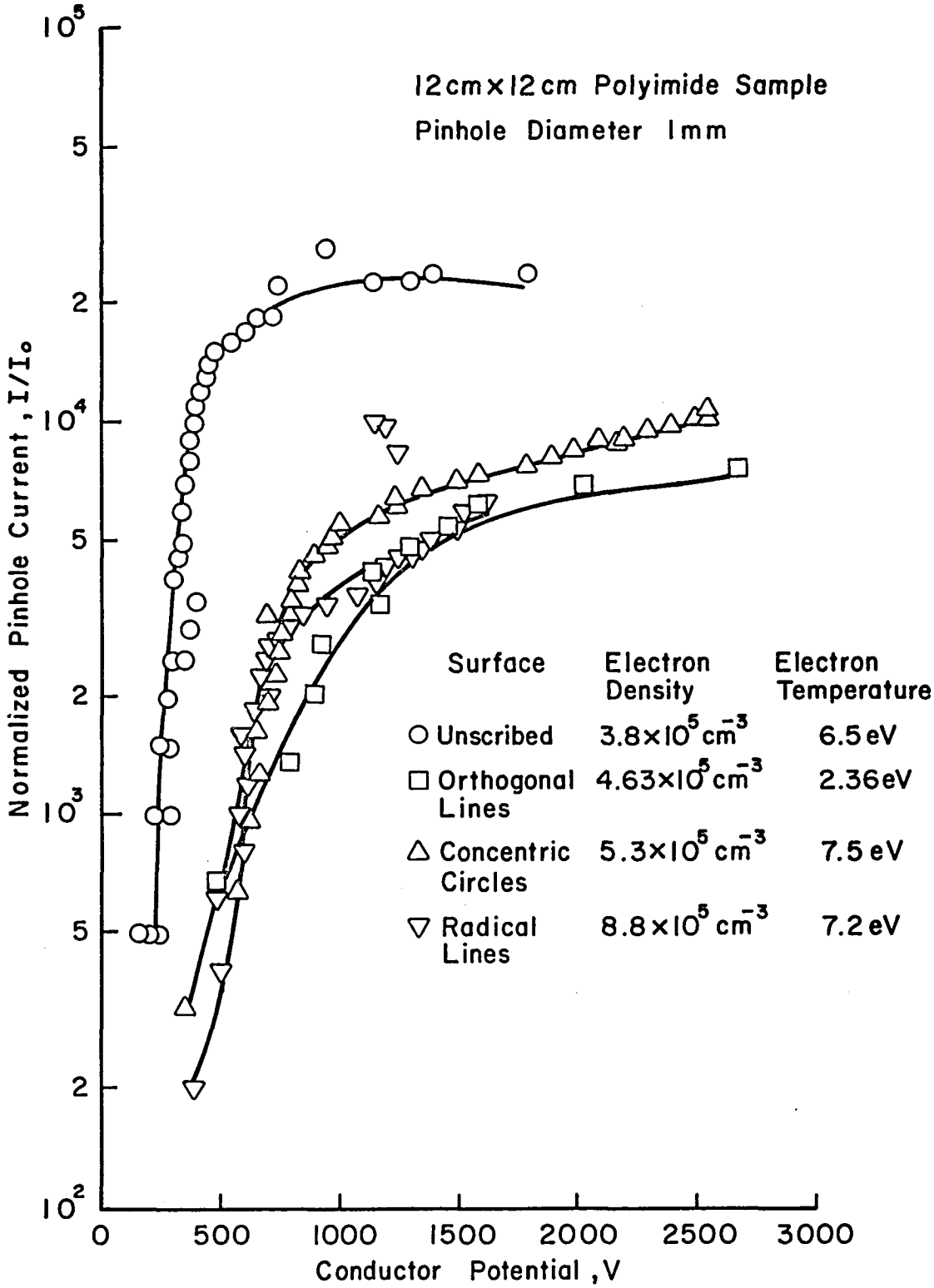

Fig. 3-19. Comparison of a plain polyimide surface sample with samples whose polyimide surface has been scribed.

To test this model, a glass-insulated sample was constructed. Glass was chosen for inertness and reduced adsorption of gases. Using a glass-insulated sample, the possibility of producing a conductive vapor near the pinhole should be reduced if the vapor comes from the bulk of the material.

The glass sample was constructed from 2.5 × 7.5 cm microscope slides of 1 mm thickness. The slides were assembled to form a 12 × 12 cm sample using polyimide tape of 1.2 cm width (see Fig. 3-20) and a 1 mm diameter pinhole was drilled in the center slide. The polyimide tape used in assembling the slides was against the pc board, so that the plasma was only in contact with glass.

In comparing the voltage-current characteristics of a glass sample with a polyimide sample (see Fig. 3-21), it was found that the glass sample conducted approximately the same current as that of the polyimide sample. From Fig. 3-21 it can also be seen that a second test yielded much lower currents and the current abruptly stopped. To investigate why the current ceased in this second test, the underlying conductor was cleaned and the test repeated (see Fig. 3-22). This resulted in a current-voltage curve similar to that of the first test.

The current cessation shown in Fig. 3-21 was typical of other glass slide tests and differs significantly from the current reduction observed with the polyimide samples. In the polyimide samples, changes in the pinhole itself seemed to cause the reduction in current, while there were no apparent effects due to the conductor underneath. With the glass samples, there appeared to be some process on the conducting copper surface causing current to cease, with no detectible difference in the behavior due to changes in the pinhole.

12cm × 12cm Surface Constructed from 3"× 5" Glass Slides Mounted on Fiberglass Backing Board. Joints Sealed Underneath with Polyimide Tape

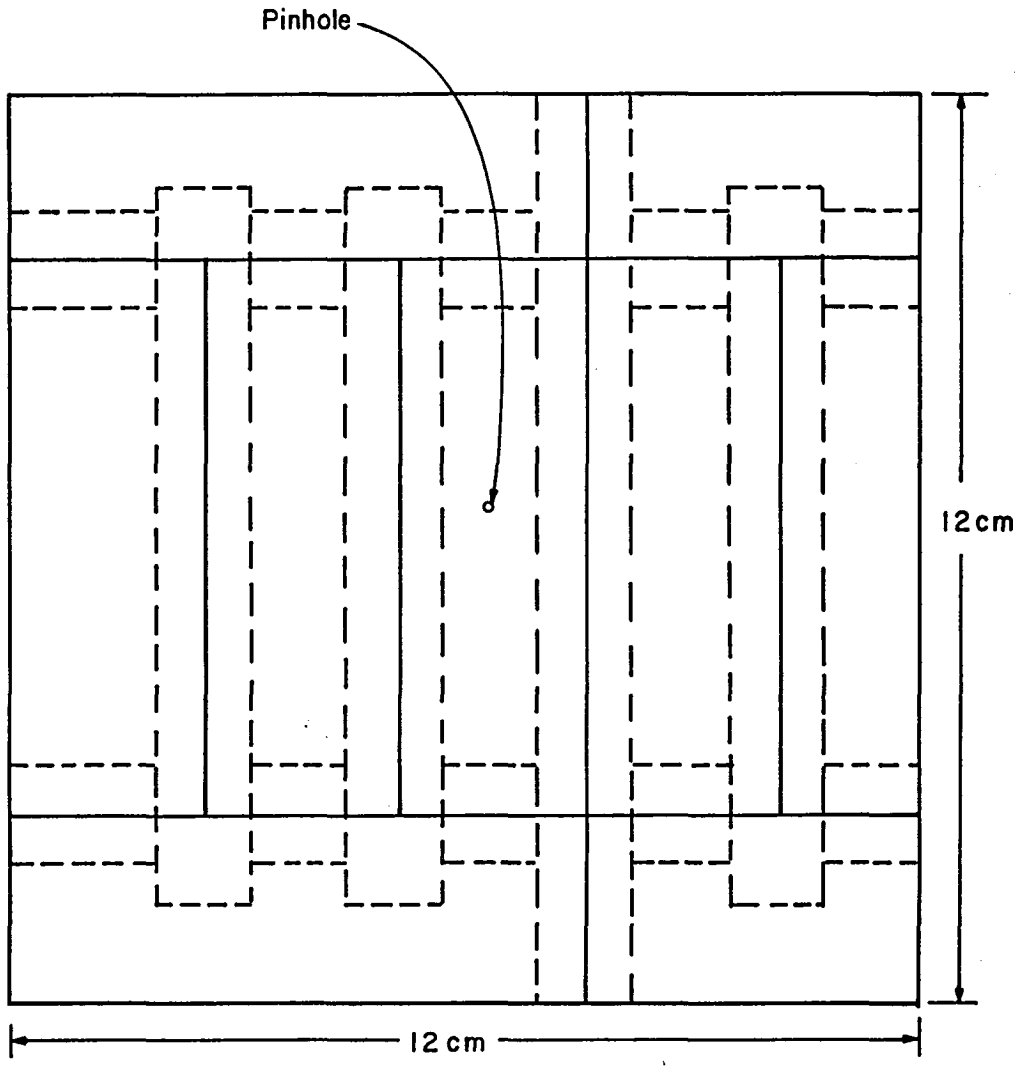

Fig. 3-20. Glass surface test sample.

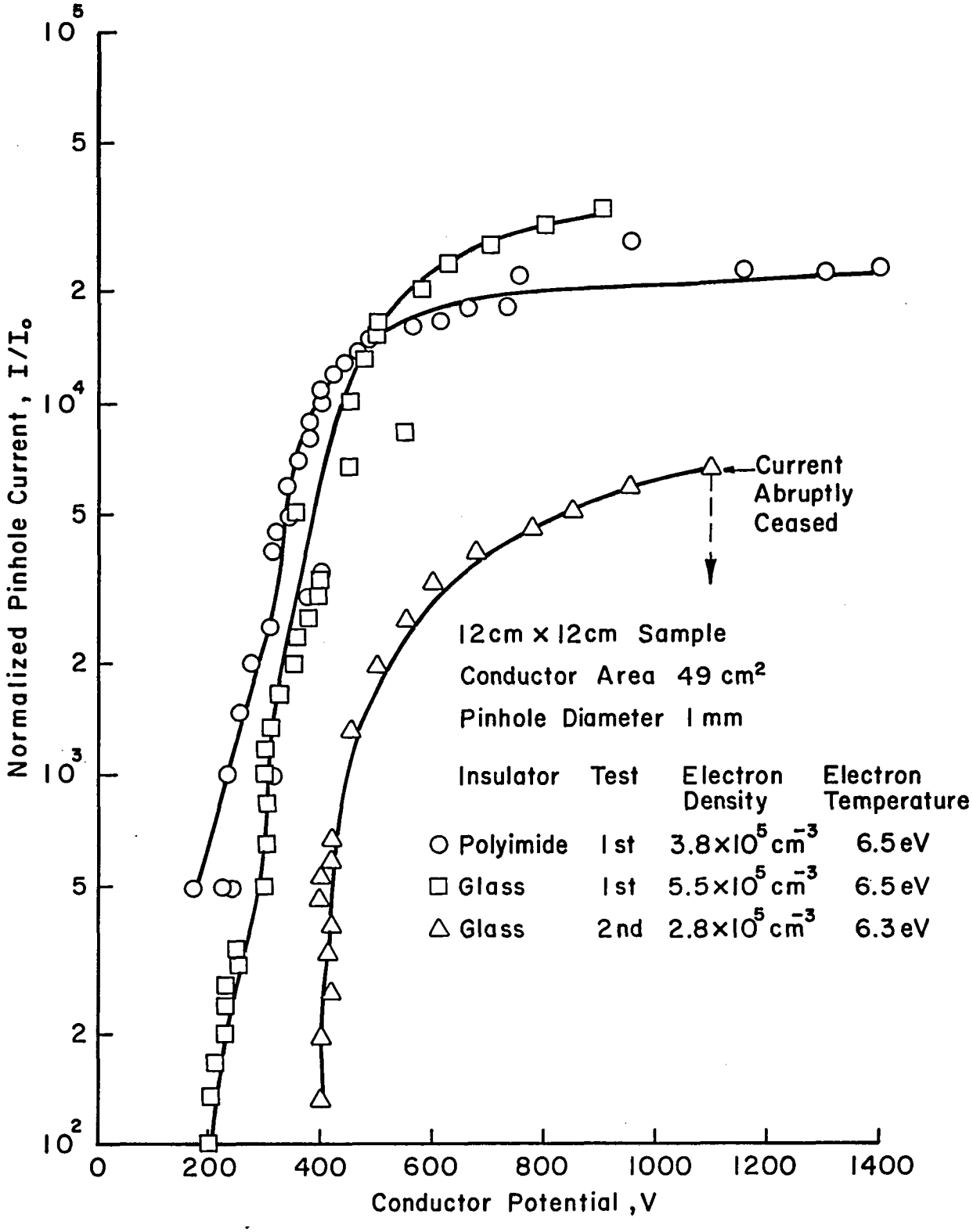

Fig. 3-21. Comparison between samples insulated with polyimide and glass.

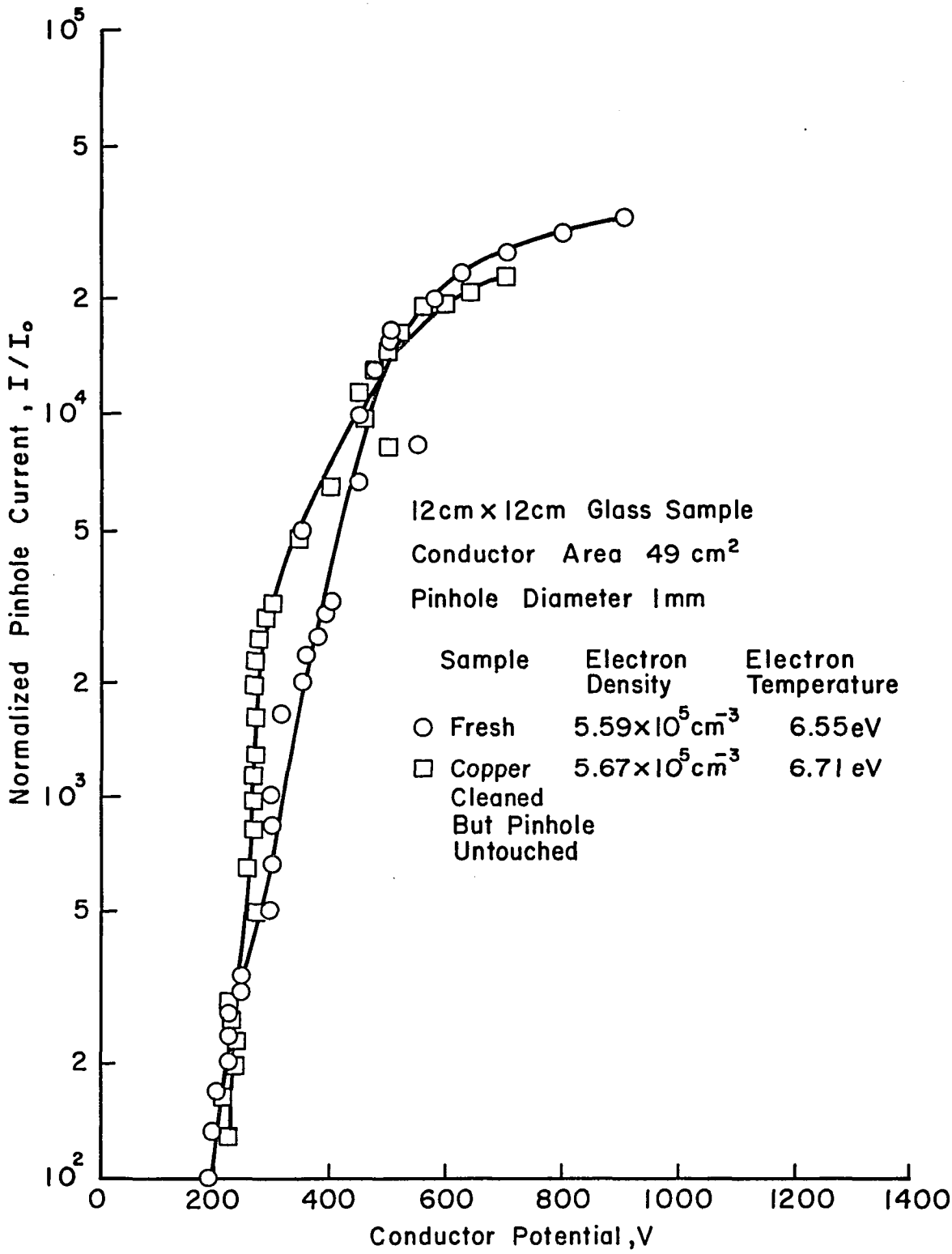

Fig. 3-22. Comparison between a fresh glass sample and a glass sample whose conductor beneath the pinhole has been cleaned.

It appeared possible that vaporized glass deposited onto the copper conductor beneath the glass, insulating the conducting copper and preventing current flow. To see if current conduction could be restored, a sample was taken to the point where current ceased, then the voltage was increased until current conduction (>1 mA) was restored. When the voltage was decreased, the conduction stopped again. This test was repeated six times on the same sample (see Table 3.2). From Table 3.2 it can be seen that the voltage needed to restore current conduction generally increased with each attempt. A possible explanation is that more insulating material was deposited on the copper with each test. Attempts to measure the resistance of the coating on the copper with an ohmmeter were inconclusive, but problems have been encountered before measuring the resistance of very thin films in this manner.

Mica. A 12 × 12 cm square of inorganically bonded (6E78300) mica was used as an alternate insulating material. The current-voltage characteristics of the pinhole in the mica insulation showed the same general shape as that of polyimide but differs in level of current reached (see Fig. 3-23).

Silicon. The next alternate material used to insulate the simulated solar cell was crystalline silicon of unknown purity, but extremely high resistivity. The sample consisted of 7.9 cm radius wafer and 0.39 mm thick. A 1 mm diameter hole was machined into the center of the wafer which was then placed on a 12 × 12 cm printed circuit board with a 6.15 cm diameter copper conductor beneath the wafer. The wafer was attached to the pc board by polyimide tape (see Fig. 2-34).

The silicon insulated test sample yielded significantly different data than any previous material used. On the first through third tests,

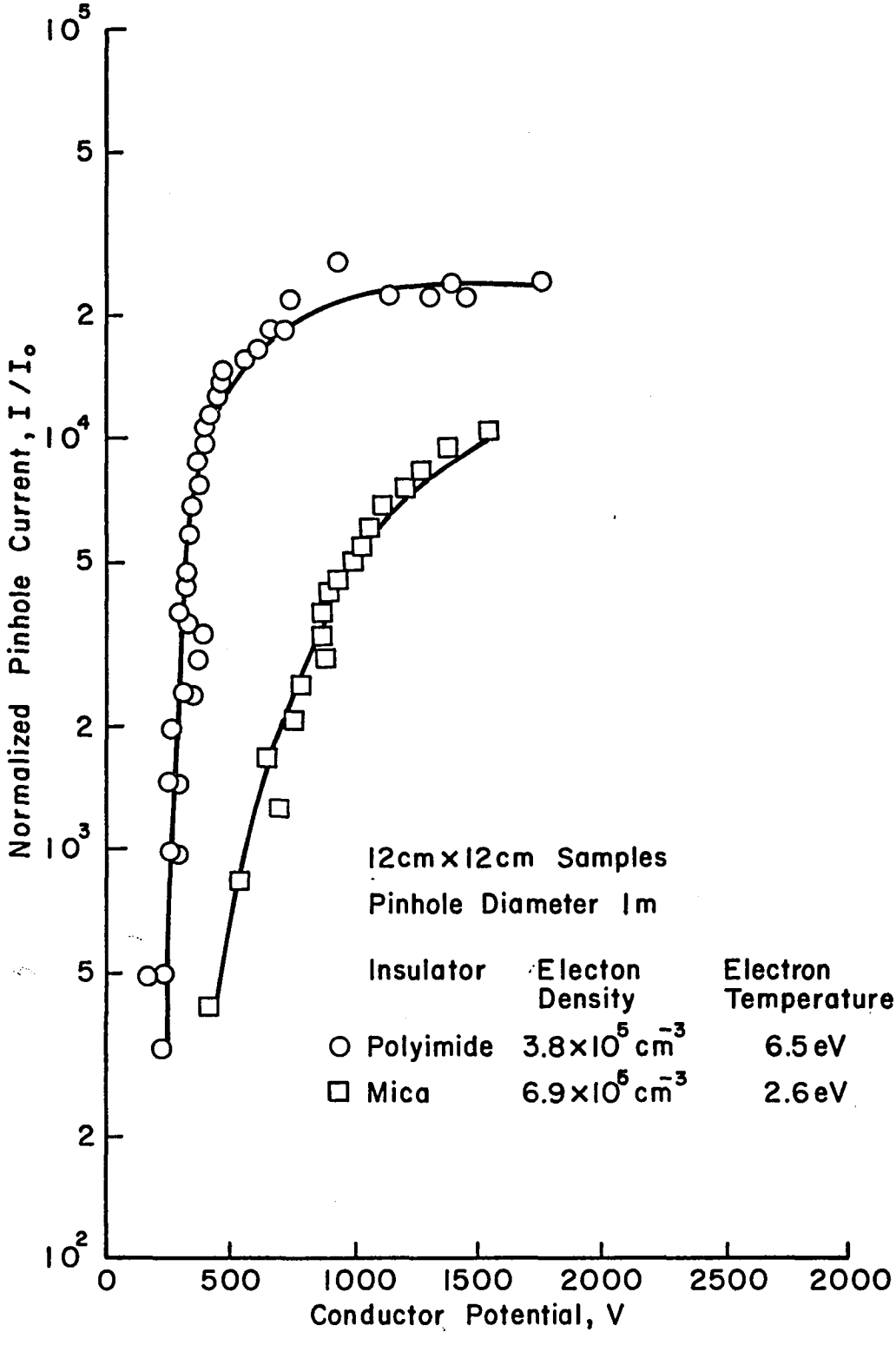

Fig. 3-23. Comparison between samples insulated with polyimide and mica.

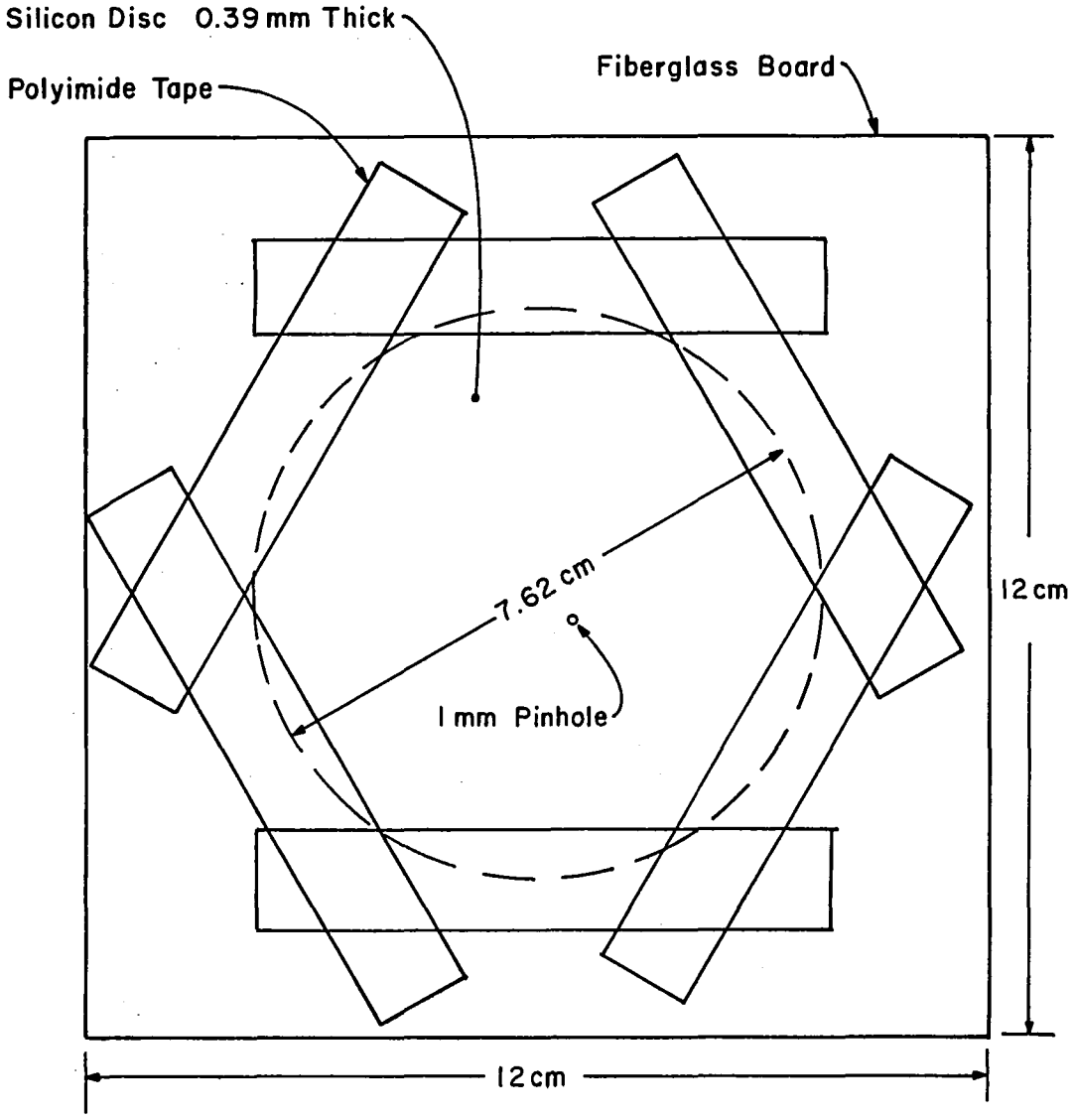

Fig. 3-24. Sketch of silicon covered test sample mounting.

Table 3.2. Voltage Needed to Restore Current Conduction through Pinhole in Glass Sample.

Test	Voltage Needed to Restore Conduction of Current (>1 mamps)
1st	7000 volts
2nd	8200 volts
3rd	8000 volts
4th	9000 volts
5th	9000 volts
6th	9500 volts

no current was observed until the voltage reached 1000 volts (see Fig. 3-25). In the area of 1000-1100 volts, the current showed a sharp but controllable increase. On the fourth test, as shown in Fig. 3-26, there was a dramatic change in the voltage-current characteristics. The voltage at first reached a high level similar to that shown in Fig. 3-25, but then dropped to a low level that was maintained as current was decreased. On the fifth and subsequent tests (see Fig. 3-27) the high currents were consistantly obtained at low voltages. This abrupt change in current-voltage characteristics may have been due to unknown current conduction in the silicon.

Effects of Multiple Pinholes

The objective of these tests was to examine the effects of multiple pinholes in polyimide insulation. Four test samples were prepared with

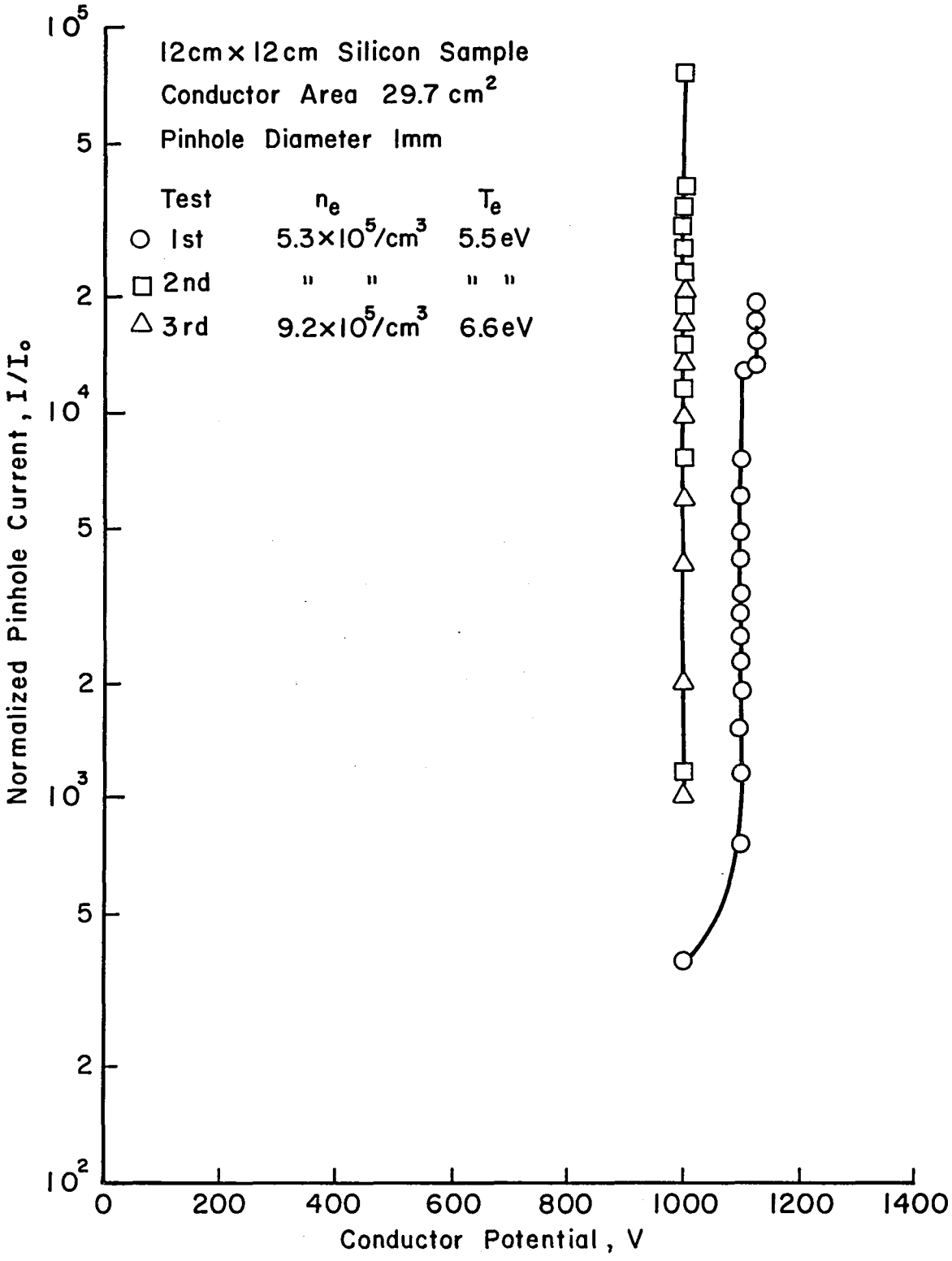

Fig. 3-25. First three tests of silicon covered sample.

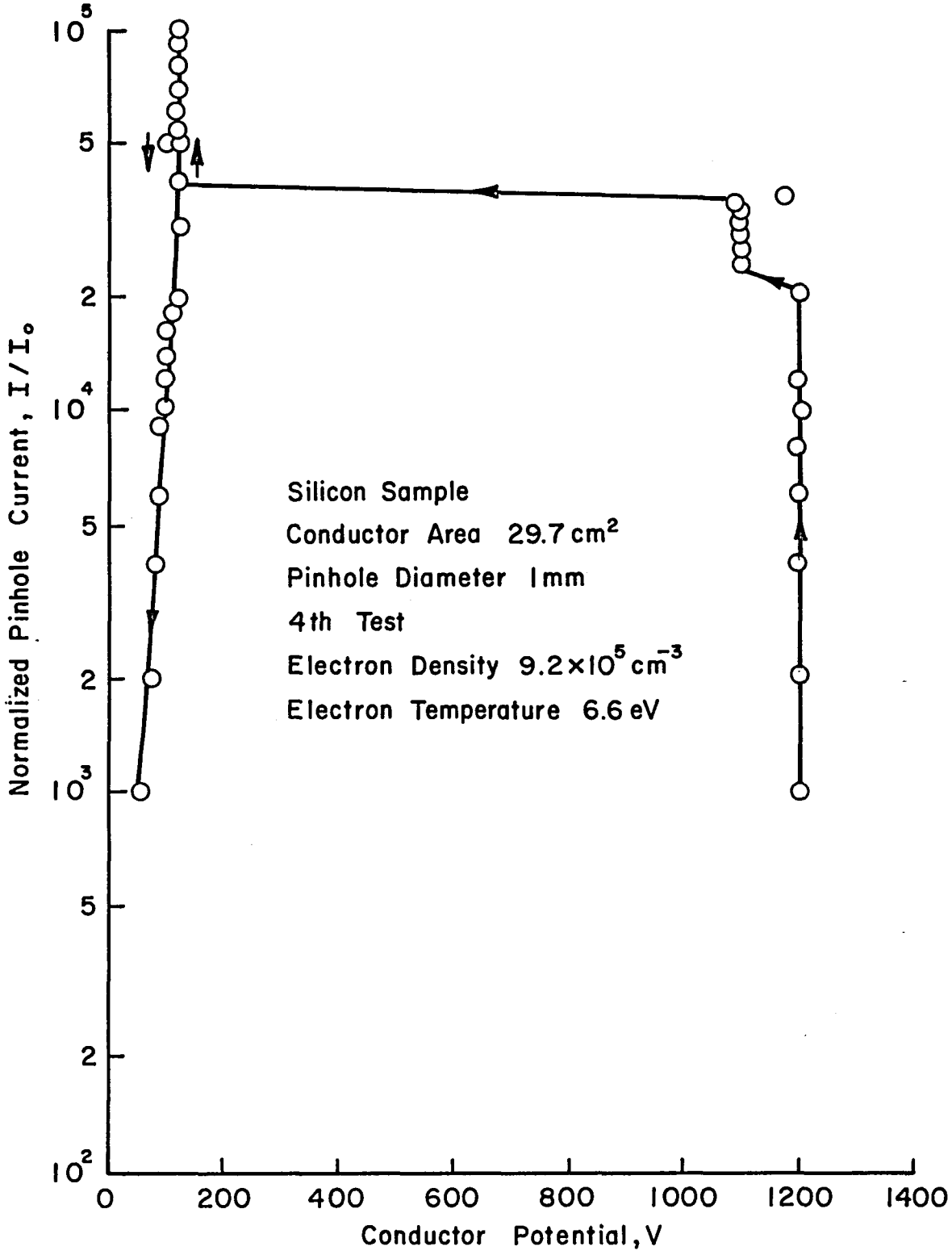

Fig. 3-26. The fourth test of the silicon covered sample.

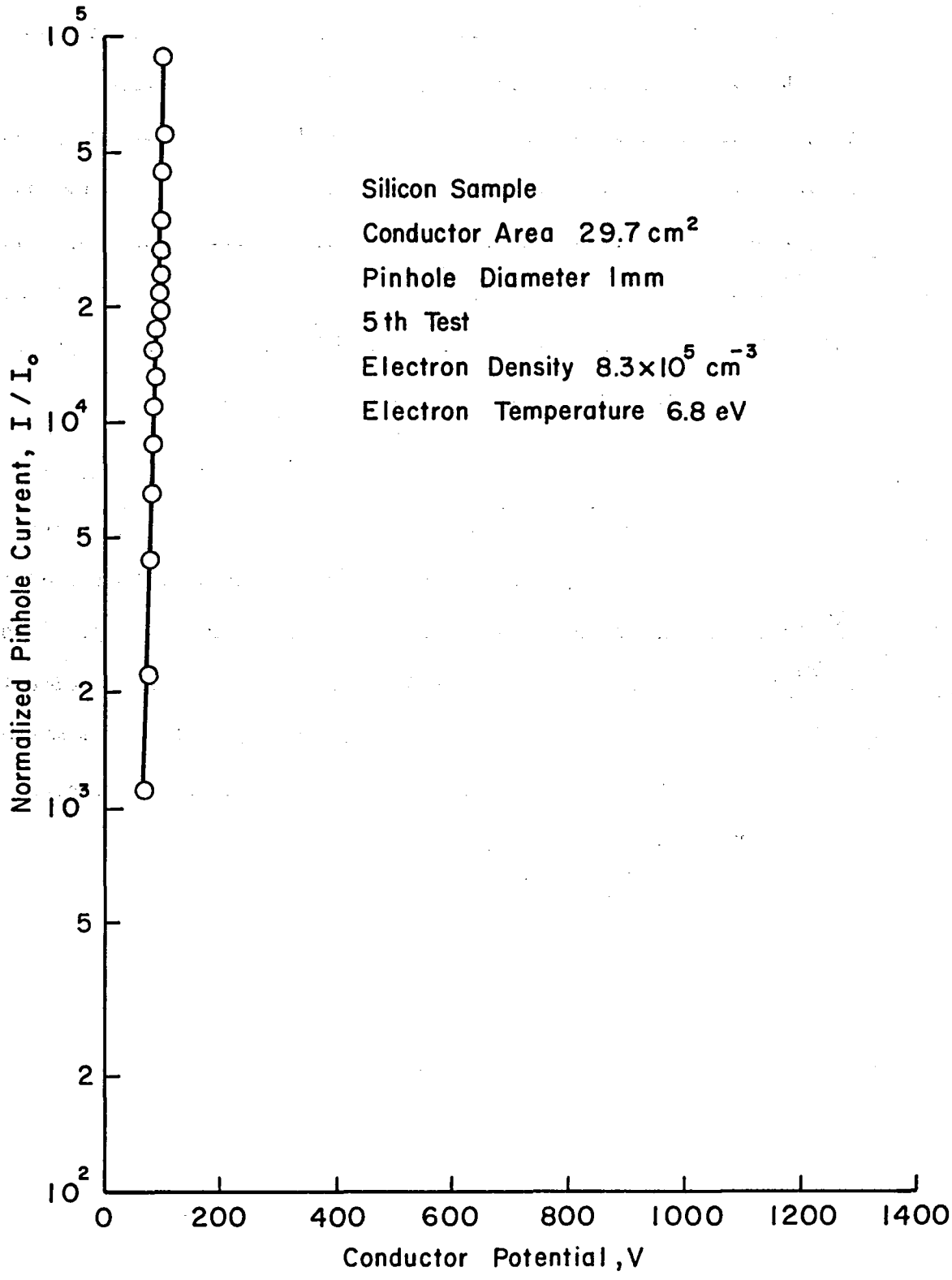

Fig. 3-27. The fifth test of the silicon sample.

two pinholes drilled in the polyimide insulation of each sample. The pinholes were separated by distances of 1/2, 1, 2, and 3 cm.

The normalization factor, I_o, was adjusted by a factor of 2 because of the doubled area of the exposed conductor through the two pinholes. This normalization resulted in the current-voltage characteristics (Figs. 3-28 to 3-31) of the two pinhole tests to be nearly superimposed on the current-voltage characteristics of the one-hole control sample. This result seems to indicate that the current collected is proportional to the total pinhole area.

Effects of Electron Extraction on Plasma Density

These tests were performed to determine what effects the extraction of electrons had on the plasma density. These tests were performed by placing a Langmuir probe in several different positions relative to the pinhole and varying the current collected by the pinhole. The results of these tests are given in Table 3.4. It can be seen that closer to the pinhole there are larger effects on density due to the increased collection of electrons.

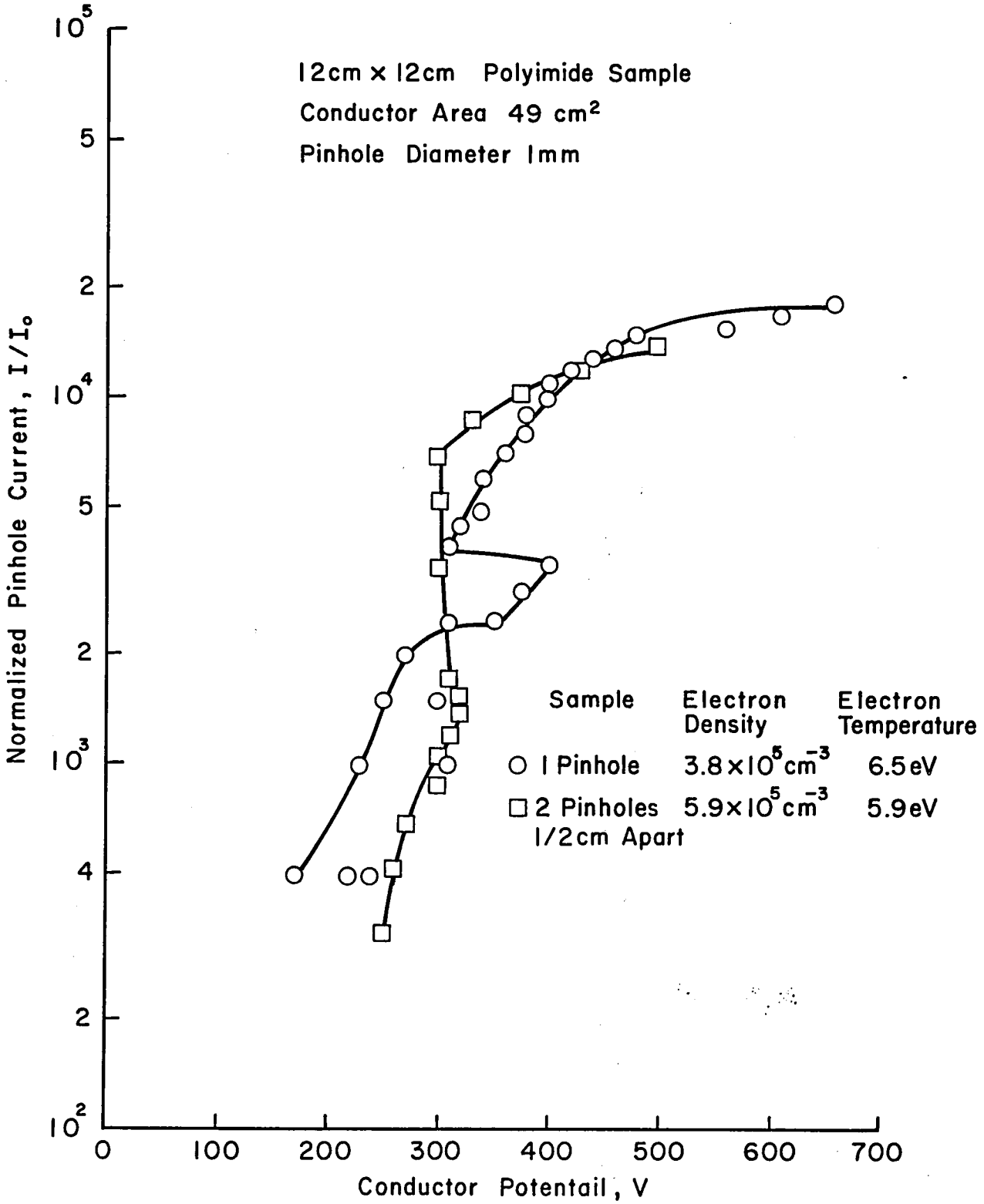

Fig. 3-28. Comparison of one pinhole with two pinholes 0.5 cm apart.

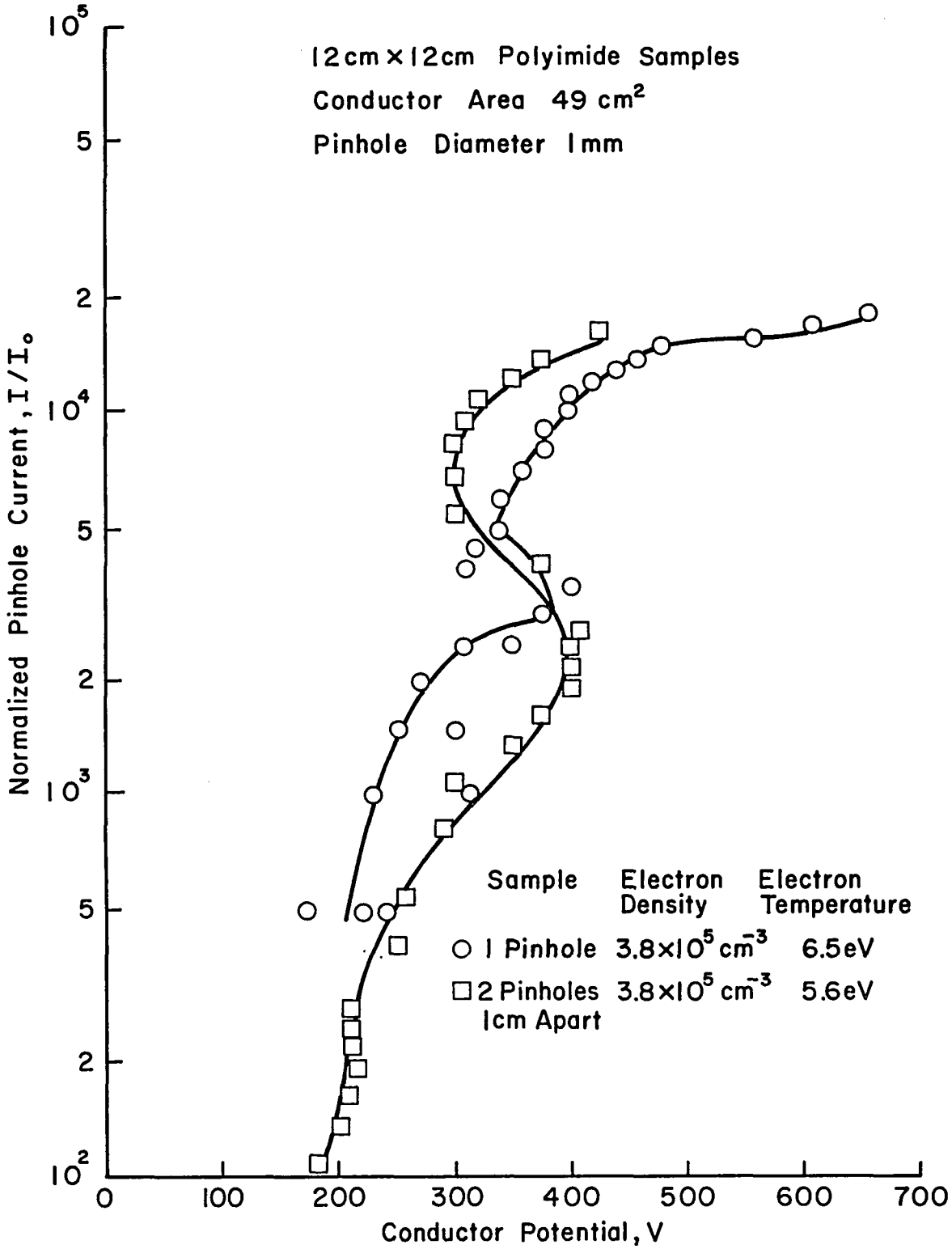

Fig. 3-29. Comparison of one pinhole with two pinholes 1 cm apart.

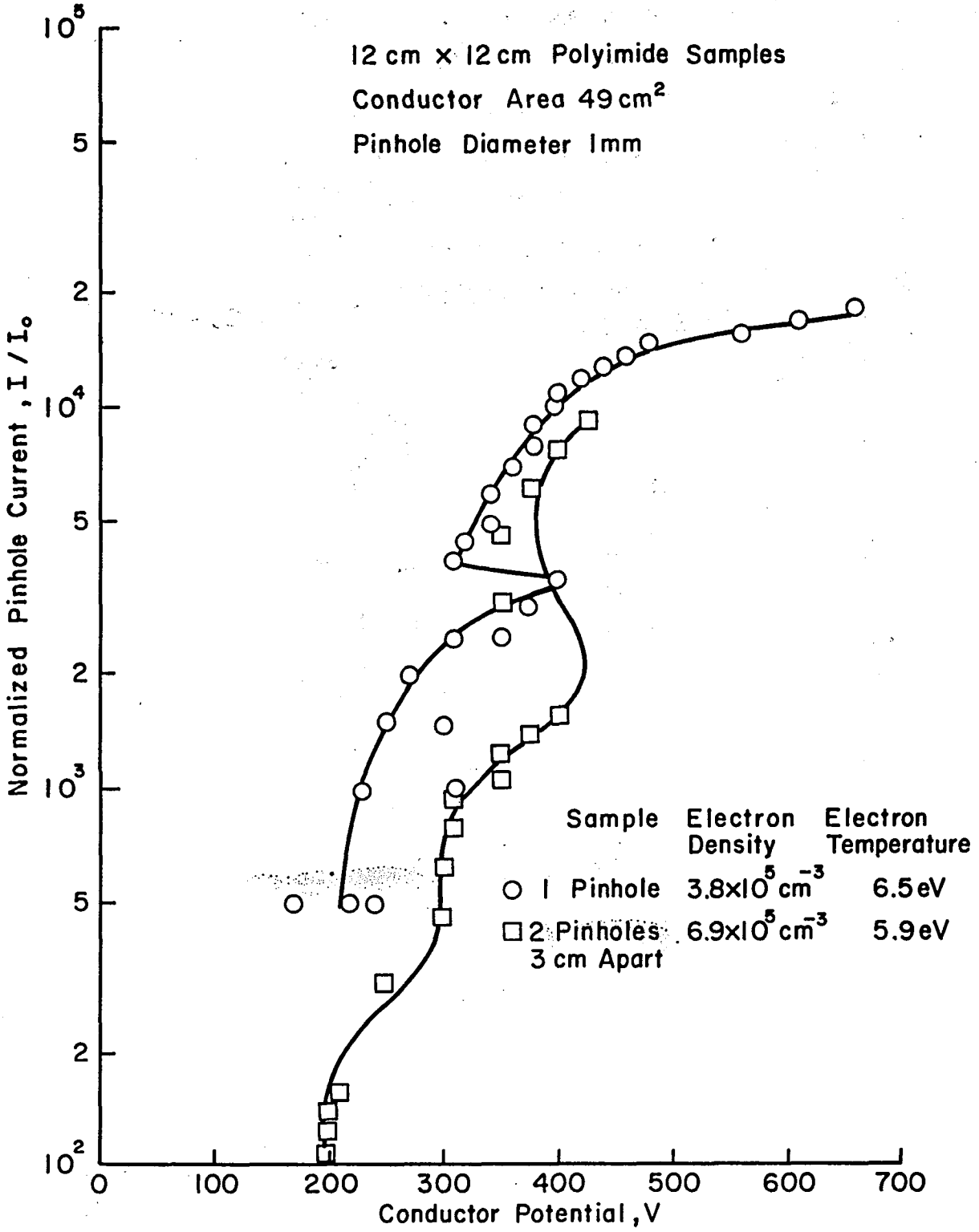

Fig. 3-30. Comparison of one pinhole vs. two pinholes 2 cm apart.

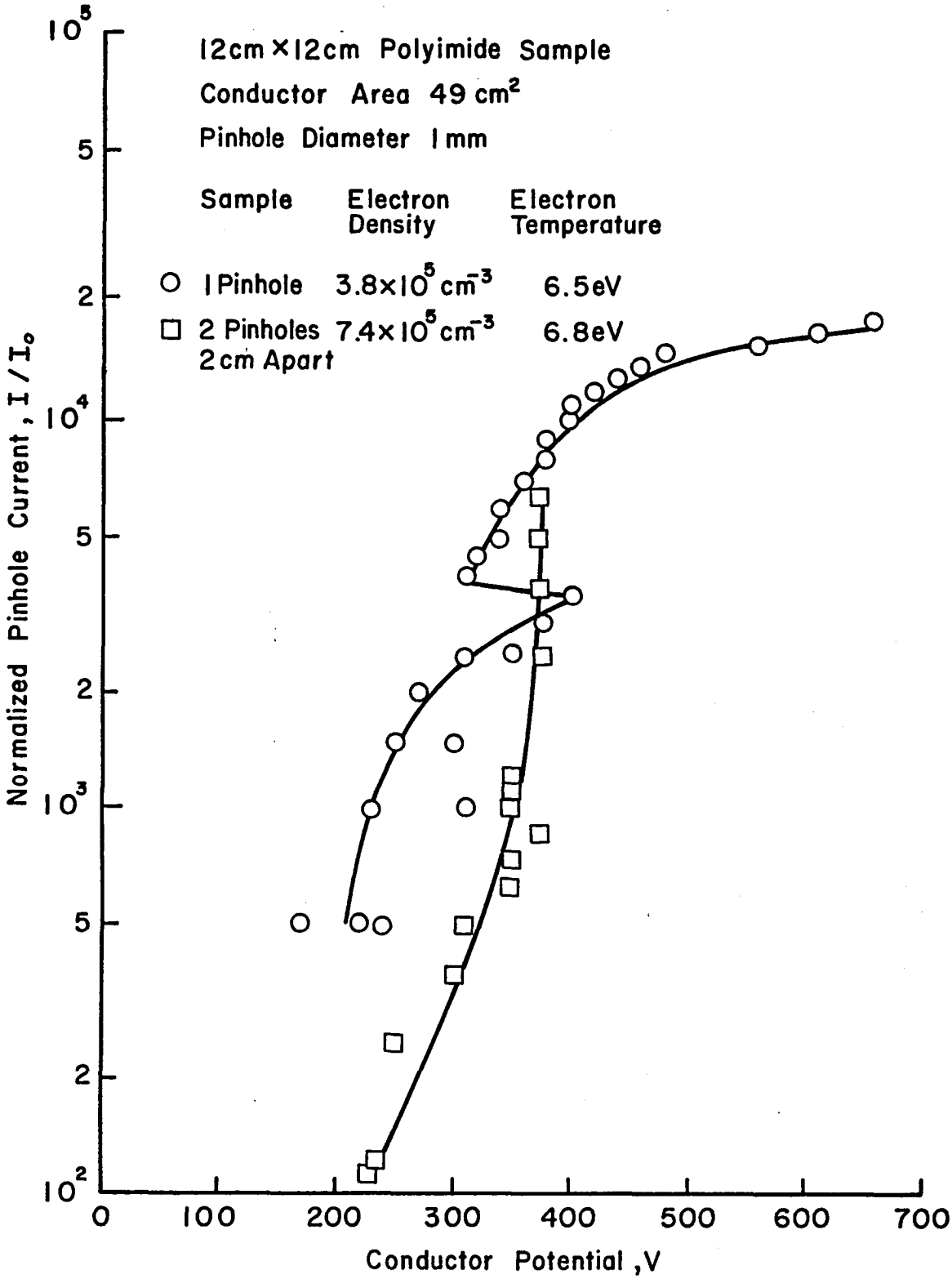

Fig. 3-31. Comparison of one pinhole and two pinholes 3 cm apart.

Table 3.4. Variation of Electron Density with Respect to Position and Current Collected by Pinhole.

Position*	Collection Current	Plasma Density
(1 cm, 0)	0 amps	$3.18 \times 10^5/cm^3$
(1 cm, 0)	50 μ amps	$2.01 \times 10^5/cm^3$
(1 cm, 0)	100 μ amps	$6.64 \times 10^4/cm^3$
(1 cm, 1 cm)	0 amps	$3.36 \times 10^5/cm^3$
(1 cm, 1 cm)	80 to 120 μ amps (oscillation)	$1.64 \times 10^5/cm^3$
(1 cm, 1 cm)	250 μ amps	$6.64 \times 10^4/cm^3$
(1 cm, 1 cm)	300 μ amps	$4.15 \times 10^4/cm^3$

*Distance from surface of sample, radial distance from axis of pinhole.

IV. DISCUSSION

Over the range of voltages investigated, the simple electrostatic effect (conducting shield around positive collection area) is limited to about 10 times the random electron arrival rate. In comparison, an insulator around the hole can result in collection currents up to 1000 times the random electron arrival rate. These results are qualitatively similar to those reported before. The major problem is, of course, the cause of this current enhancement. The most promising explanation, corresponding to the results of Kennerud,[1] is that the insulator area around a hole is responsible for this current enhancement. One possible physical explanation is that secondary electron emission at high enough electron energies permits an effective surface conduction along the insulator surface.

The tests reported herein simply do not support the "area effect". Not only were different insulator areas used around the holes, but also two holes were spaced different distances apart in these tests. The general conclusion that can be drawn is that any area effect for these tests must occur at a radius of less than 1 cm from the hole. This conclusion should be tempered with the observation that a saturation effect may be masking some of the possible area effect (see p. 30).

To reconcile this observation with the results reported by Kennerud, the experimental conditions should be examined. In those experiments the sample support had a conducting rim around it, while most samples used herein had plain edges without conductor. Another difference was the use of adhesive. Kennerud used an adhesive for the insulating sheet right up to the edge of the hole, while the adhesive herein was at least 1/2 cm from the hole. Another difference was in the area of conductor

behind the insulator. We tested the effect of the presence or absence of a conducting rim herein, but found no significant difference. Also, the effect of adhesive close to the hole should not result in a variation due to insulator area far from the hole. Different areas of underlying conductor were also tested and had no significant effect. There was one other difference that does appear to be significant. The plasma densities in Kennerud's tests were about a factor of 10 lower than the tests herein. The neutral density difference may also be significant and was $\sim 10^{11}$ cm^{-3} of nitrogen in Kennerud's tests and $\sim 10^{12}$ cm^{-3} of argon in the tests herein.

The most likely cause for the difference, then, is the difference in plasma environment, with the difference in neutral density a possible contributing factor. A related conclusion that there is the implication that different mechanisms are involved in different operating regimes. A combination of mechanisms is, of course, more difficult to unravel than one simple mechanism.

A major effect of repeated tests on collected current was found in the investigation reported herein. This effect was apparently not noted previously, although the material involved in the first tests (polyimide) had been used in previous tests. This "aging" effect of polyimide appears to be associated with the condition of the insulator surface on the inside of the hole. Adsorbed gas layers were not indicated as a factor. Instead, the generation of vapor from small projections from the initially rough drilled surface probably enhanced local vapor density during current collection. The enhanced vapor density, in turn, resulted in increased plasma density and therefore current collection. Repeated tests appeared to smooth out the polyimide surface and thereby reduced

current collection at a given voltage. No indication of an insulating layer being deposited on the conductor was found.

Tests with glass insulation gave substantially different results. No "aging" effect of repeated tests was found for the glass insulator. Instead, the repeated tests appeared to result in a layer of glass being deposited on the conductor. Note that this effect differs sharply from tests with polyimide.

Another material effect was observed with mica insulation, with lower first-test collection currents being observed than with either polyimide or glass. This result is consistent with vapor generation being a significant factor, and a higher temperature material generating less vapor with the same electron bombardment.

The results with a silicon insulator were different from those with any of the other materials. At this time, the different results with silicon appear attributable to the semiconductor nature of the material.

Fairly clear indications of an area effect, presumably due to surface interactions, were found by Kennerud. It would be surprising if some related phenomena were not observed in this investigation. Scribed surface patterns on the polyimide surface showed a general tendency to lower the collected current at a given voltage level. Various conductor patterns were tried, but the only one that significantly affected the current collection (by decreasing it) was a 2 × 2 cm mesh on the insulator surface.

The effects of both surface scribing and a conducting mesh were limited to a factor of several. It should be noted, though, that this magnitude of improvement was found at a plasma density where area affects were small. At lower plasma densities, one might expect the effects of

surface treatment to be much larger. In the absence of both experimental verification and a sound theoretical understanding of phenomena involved, however, the effect of surface treatment at lower plasma densities must be considered speculation.

It should be noted that there are some contradictions of the surface effects indicated above with the other data interpretations given previously. For example, holes being as close as 0.5 cm did not appear to reduce the current collection of each. This indicates, of course, no surface effect outside of a radius of 0.5 cm. On the other hand, the 2 × 2 cm conducting mesh had an effect with the mesh no closer than 1 cm from the hole. This latter effect indicates that some sort of effect can, indeed, take place due to a surface change outside of a 0.5 cm radius from the hole. No resolution of this contradiction is evident at this time. It may be that the data scatter noted earlier casts doubt on the interpretations given.

Some of the data scatter and variation in supposedly duplicate tests is probably due to variation of one or more important, but ignored, variables. One such variable is probably temperature. The generation of vapor has been shown fairly conclusively to be a significant factor in the investigation reported herein. The generation of vapor can often be affected by temperature. Further tests should therefore include sample temperatures.

The apparent differences due to plasma densities should also be investigated further. If the importance of different current enhancement mechanisms shifts with plasma density, then predicting effects by scaling will be difficult for different densities.

V. CONCLUDING REMARKS

Surface-area effects were found to be substantially reduced from those previously reported at lower plasma densities. The difference in typical plasma density was felt to be the major cause of this change, although a saturation effect may also be involved. At the $10^5/cm^3$ plasma density range of this investigation, surface effects on collection current appear limited to roughly 1 cm from the hole.

A factor of several reduction of collected current was obtained with both surface scribing and a 2 × 2 cm conducting mesh. It appears possible that the effects of surface treatment might be more significant at lower plasma densities.

Effects of repeated tests were also noted, with current collection decreasing with successive tests. Depending on the materials involved, the effect appeared due to either the smoothing of the inside of the insulator hole or the sputtering of insulator on the exposed conductor.

A general conclusion was made from a variety of observations, that the generation of vapor was a major factor in the enhancement of collected current. Because of the importance of vapor generation, future studies should include sample temperature variation.

APPENDIX A

Spherical Probe Analysis

The method used to analyze the data from the Langmuir probe, for thick sheaths, involves two regions of the current-voltage characteristics of the probe. The two regions are the transition and attracting regions of the curve.

Transition Region. The probe is charged negatively to repel electrons, if the electron distribution is in thermal equilibrium, then the density follows Boltzmann Law

$$n = n_o \exp\ (-V/T_e) \tag{A-1}$$

where n = electron density (in cm^{-3}), V = probe voltage (in eV), T_e = electron temperature (in eV), and n_o = normalization constant. Since the distribution is Maxwellian, only the density is changed by the potential.

The random current hitting the probe is

$$I = A_p j \tag{A-2}$$

where I = current striking the probe, A_p = probe area, and j = electron current density. For a Maxwellian distribution,

$$j = \frac{1}{2}\, ne \left(\frac{2T_e}{\pi m_e}\right)^{1/2} \tag{A-3}$$

where m_e = electronic mass. Plotting lnI versus V (see Fig. A-1 for sample curve)

$$T_e = \text{slope}^{-1} = \Delta V/\Delta \ell nI \tag{A-4}$$

Attracting Region. To find the electron density, the attracting region is used. For a thick sheath analysis, orbit limited theory is employed. The current collected by the probe is given by[1]

$$I = A_p j \ (1 + V/T_e) \tag{A-5}$$

$$\frac{dI}{dV} = \frac{A_p j}{T_e} = A_p ne \ [2 \ m_e T_e]^{-\frac{1}{2}} \tag{A-6}$$

or

$$n = \frac{[2\pi m_e T_e]^{\frac{1}{2}}}{A_p e} \ \frac{dI}{dV} \tag{A-7}$$

for $A_p = .51\frac{1}{2}cm^2$ (see Fig. A-2 for sample curve).

$$n = 7.40 \times 10^{10} \ T_e^{\frac{1}{2}} \ \frac{dI}{dV} \ cm^{-3} \tag{A-8}$$

Plasma Potential. To calculate plasma potential, data from both regions are employed. In the transition region

$$I = I_o \exp \ (V/T_e) \ . \tag{A-9}$$

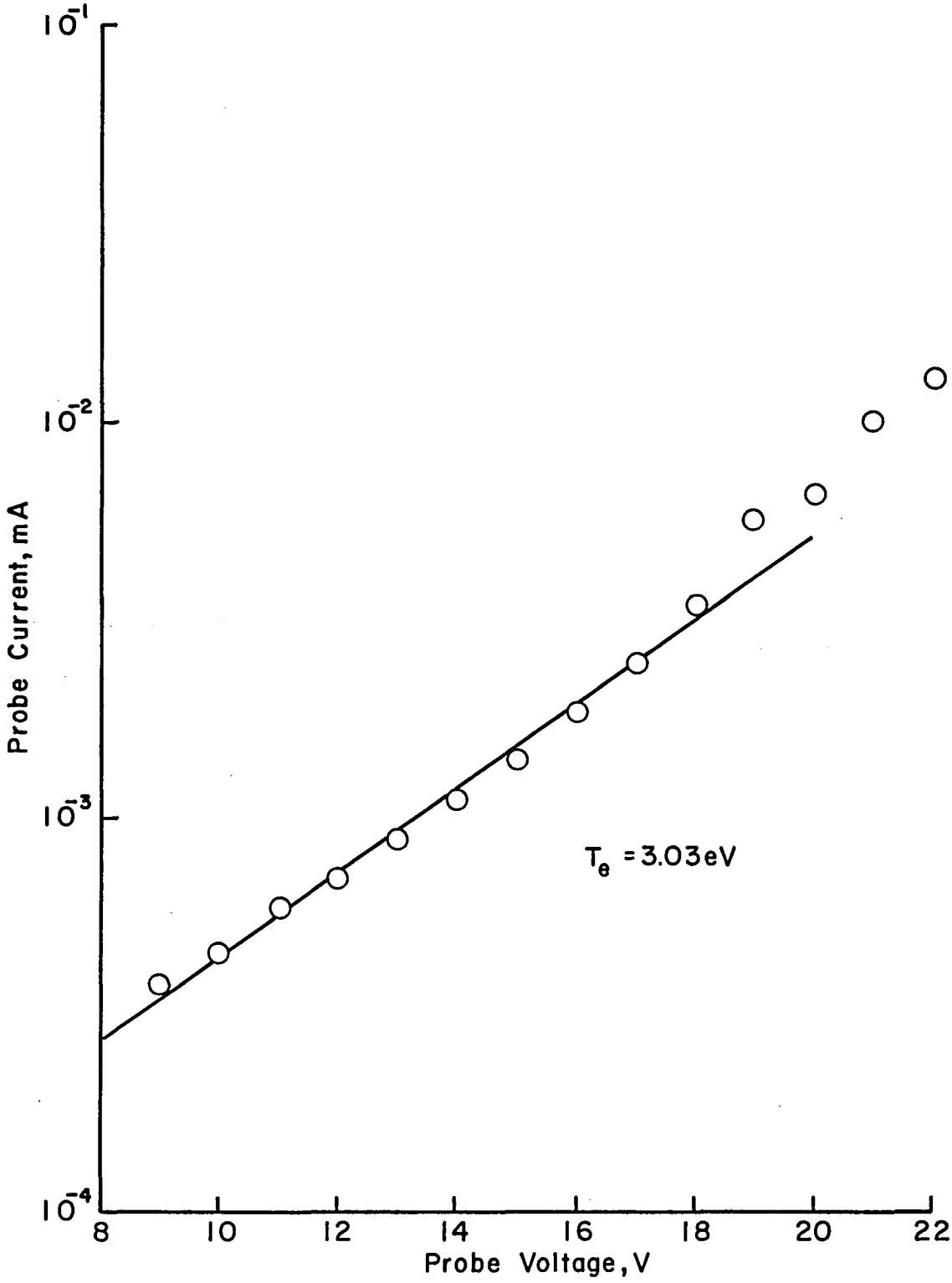

Fig. A-1. Probe current-voltage characteristic in transition region.

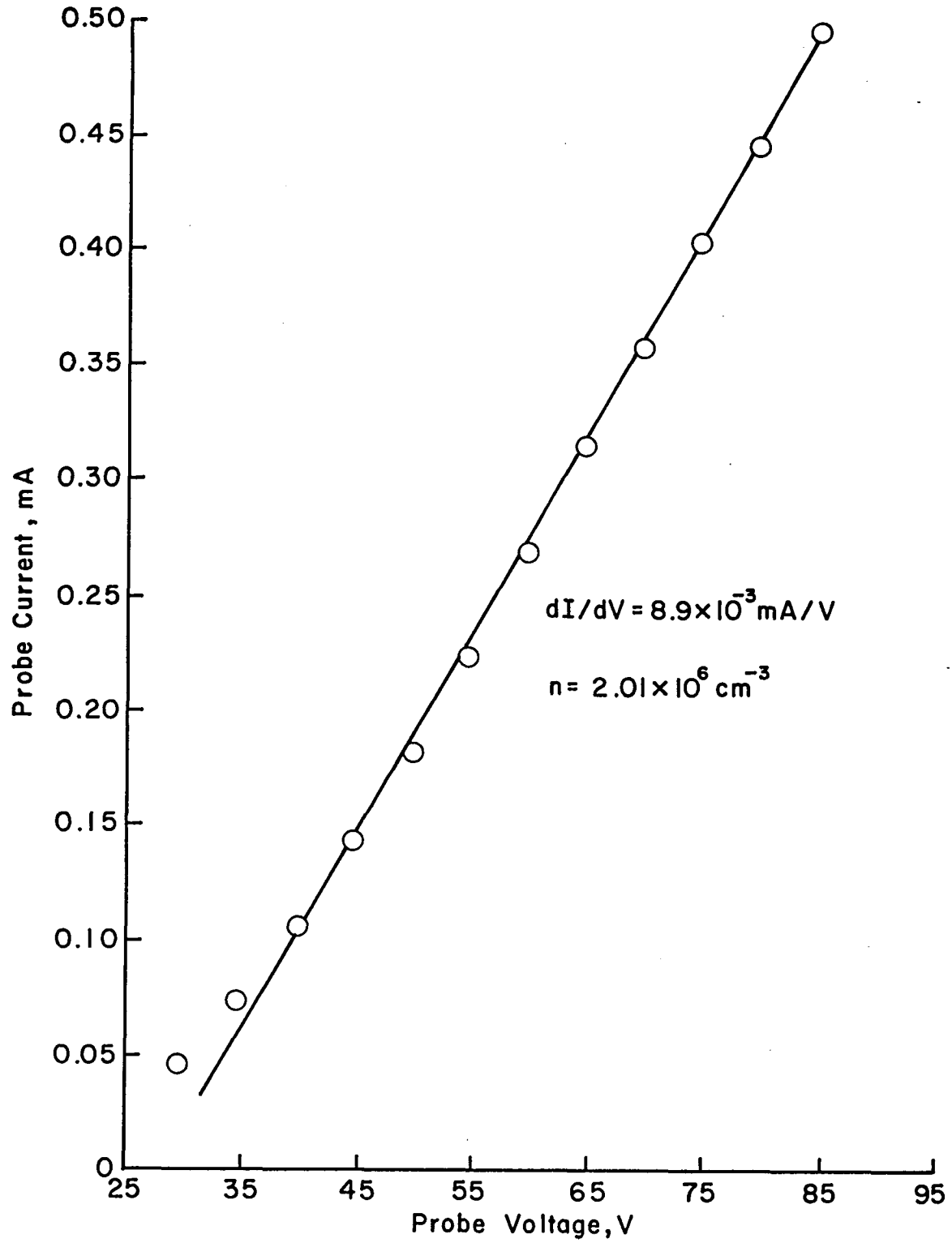

Fig. A-2. Probe voltage-current characteristic in attracting region.

Let I_1 be some current in the transition region.

$$I_o = I_1 \exp(-V_1/T_e) \quad . \tag{A-10}$$

At $I = I_{sat}$; $V = V_p$, where I_{sat} = saturation current, V_p = plasma potential. Then

$$I_{sat} = I_1 \exp(-V_1/T_e) \exp(V_p/T_e) \tag{A-11}$$

or

$$V_p = V_1 + T_e \ln I_{sat}/I_1 \tag{A-12}$$

where

$$I_{sat} = en A_p (T_e/2\pi m_e)^{\frac{1}{2}} \quad . \tag{A-13}$$

APPENDIX B

Planar Probe Theory[1]

The geometry of the probe is shown in Fig. B-1. In this theory, the probe potential (V_o) is referenced to the plasma potential, and the probe is flush with a conductor.

In the sample holder, the conducting area surrounding the pinhole is equivalent to the conductor surrounding the planar probe.

The equation describing the current collection of this planar probe is

$$I = I_o \left\{ 1 + \frac{V_o}{T_e} - \frac{b^2}{4} \left(\frac{V_o}{T_e} \right)^2 \exp\left(\frac{V_o}{T_e} \right) E_1 \left(\frac{V_o}{T_e} \right) \right\} \tag{B-1}$$

where

$$I_o = Ane \left(\frac{T_e}{2\pi m_e} \right)^{1/2} \tag{B-2}$$

and

$$E_1(\chi) = \int_{\chi}^{\infty} \frac{e^{-t}}{t} \, dt \, . \tag{B-3}$$

For large values of V_o/T_e, it can be approximated by

$$I = I_o \left[1 + \frac{b^2}{4} + \left(1 - \frac{b^2}{4} \right) \frac{V_o}{T_e} \right] \tag{B-4}$$

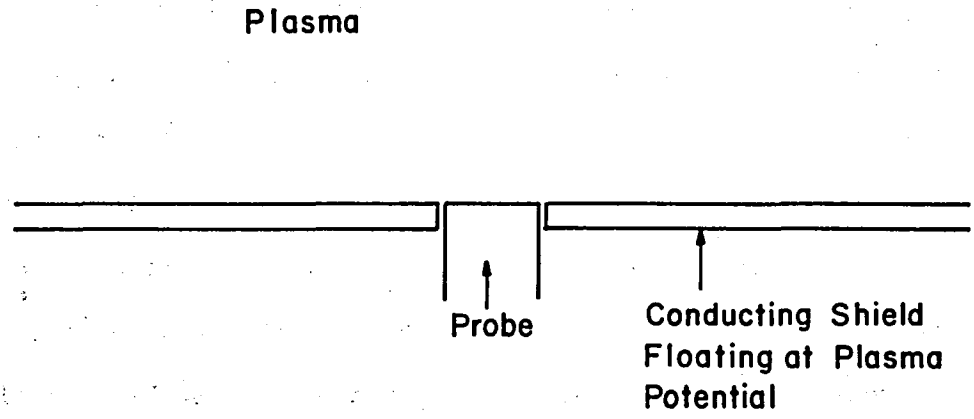

Fig. B-1. Geometry of planar probe.

where b is an adjustable parameter related to the trajectories of the incoming electrons. The constant b can range from 0 to 2.

Tests were made to determine the value of b. Figure B-2 shows two typical tests. Comparison between theoretical versus experimental values of the current-voltage characteristics are in good agreement for lower voltages, at large voltages the curves begin to separate.

One possible explanation of this behavior is that in the model describing this behavior, the applied voltage on the probe was varied, but the plasma was assumed constant. In the bell jar facility, while increasing the probe voltage, the plasma is also being depleted, which increases the Debye length, which in turn increases the plasma area from which current can be drawn. This behavior merely limits the region in which a comparison can be made between current collected from the plasma directly and current from surface effects.

Table B-1 lists the density versus the value of b and the value where the collected current deviates from the predicted values, hereafter known as V_H.

The average value of b was found to be $1.80 \pm .08$.

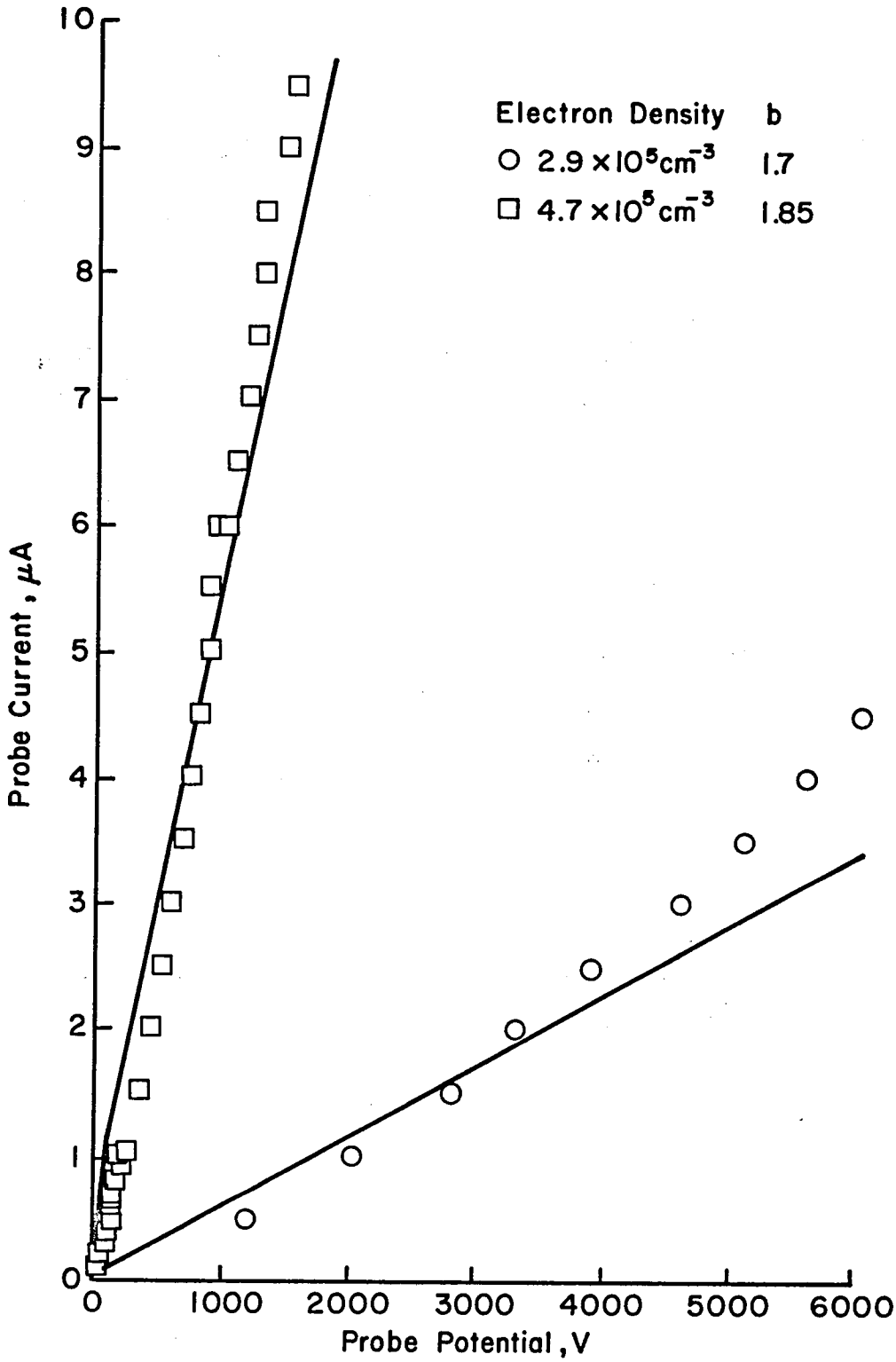

Fig. B-2. Planar probe current-voltage characteristics at two different densities.

Table B-1.

Density	b	V_H (volts)
2.97×10^5	1.70	2000
3.06×10^5	1.77	2520
4.23×10^5	1.80	2700
4.91×10^5	1.77	1600
5.35×10^5	1.77	1030
3.59×10^6	1.95	300
6.49×10^6	1.05*	>1250
4.72×10^6	1.85	1300

*Left out of calculation of average b.

REFERENCES

Section I

1. D. J. Santelir, D. H. Holkeboer, D. W. Jones, and F. Pagano, "Vacuum Technology and Space Simulation", NASA Special Publication SP-105, pp. 33-40, 1967.

2. J. A. Wolfe, in "Solar Wind" (edited by C. P. Sonett, P. J. Coleman, Jr., and J. M. Wolcox), NASA Special Publication SP-308, pp. 170-201, 1972.

3. C. R. Chappell, Rev. of Geophysics and Space Physics, Vol. 10, pp. 951-979, Nov. 1972.

4. R. K. Cole, A. S. Ogawa, and J. M. Sellen, Jr., AIAA Paper No. 69-262 (1969).

5. N. T. Grier and D. J. McKinzie, AIAA Paper No. 69-262 (1969).

6. J. R. Bayless, B. G. Herron, and J. D. Worden, AIAA Paper No. 72-443 (1972).

7. N. T. Grier and S. Domitz, NASA Tech. Note TND-8111 (1975).

8. K. L. Kennerud, NASA Contractor Report CR-121280 (1974).

Section II

1. Francis F. Chen, Introduction to Plasma Physics, New York, Plenum Press, 1977, pp. 199-202.

Section IV

1. K. L. Kennerud, NASA Contractor Report CR-121280 (1974).

Appendix A

1. F. F. Chen, "Electric Probes", Plasma Diagnostic Techniques, Huddlestone, R. H. and Leonard, S. L., editors, Academic Press, New York, pp. (1965).

Appendix B

1. L. W. Parker and E. C. Whipple, "Theory of a Satellite Electrostatic Probe", Annals of Physics 44, pp. 126-167 (1967).

DISTRIBUTION LIST

	No. of Copies
National Aeronautics and Space Administration Washington, DC 20546	
Attn: RPE/Mr. Wayne Hudson	1
Mr. Daniel H. Herman, Code SL	1
National Aeronautics and Space Administration Lewis Research Center 21000 Brookpark Road Cleveland, OH 44135	
Attn: Research Support Procurement Section	
Mr. Allen Jones, MS 500-313	1
Technology Utilization Office, MS 3-19	1
Report Control Office, MS 5-5	1
Library, MS 60-3	2
N. T. Musial, MS 600-113	1
Spacecraft Technology Division, MS 501-8	
Mr. H. Douglass	1
Mr. R. Finke	1
Mr. D. Byers	1
Mr. B. Banks	1
Mr. S. Domitz	1
Mr. Norman T. Grier	20
Mr. F. Terdan	1
Mr. W. Kerslake	1
Mr. Vincent K. Rawlin	1
Mr. M. Mirtich	1
Chief Scientist	
Mr. W. E. Moeckel	1
National Aeronautics and Space Administration Marshall Space Flight Center Huntsville, AL 35812	
Attn: Mr. Jerry P. Hethcoate	1
Research and Technology Division Wright-Patterson AFB, OH 45433	
Attn: (ADTN) Lt. David A. Fromme	1
NASA Scientific and Technical Information Facility P.O. Box 8757 Baltimore/Washington International Airport Baltimore, MD 21240	40
Case Western Reserve University 10900 Euclid Avenue Cleveland, OH 44106	
Attn: Dr. Eli Reshotko	1
Royal Aircraft Establishment Space Department Farnborough, Hants, ENGLAND	
Attn: Dr. D. G. Fearn	1

United Kingdom Atomic Energy Authority
Culham Laboratory
Abingdom, Berkshire, ENGLAND
Attn: Dr. P. J. Harbour 1
Dr. M. F. A. Harrison 1
Dr. T. S. Green 1

National Aeronautics and Space Administration
Goddard Space Flight Center
Greenbelt, MD 20771
Attn: Mr. W. Isley, Code 734 1
Mr. R. Bartlett, Code 713 1
Mr. R. Callens, Code 734 1

SAMSO
Air Force Unit Post Office
Los Angeles, CA 90045
Attn: Capt. D. Egan/ SYAX 1

Comsat Laboratories
P. O. Box 115
Clarksburg, MD 20734
Attn: Mr. B. Free 1
Mr. O. Revesz 1

Roket Propulsion Laboratory
Edwards AFB, CA 93523
Attn: LKDA/Ms. Tom Waddell 2

DFVLR - Institut für Plasmadynamik
Technische Universitat Stuttgart
7 Stuttgart-Vaihingen
Allmandstr 124
WEST GERMANY
Attn: Dr. G. Krülle 1

Giessen University
1st Institute of Physics
Geissen, WEST GERMANY
Attn: Professor H. W. Loeb 1

Jet Propulsion Laboratory
4800 Oak Grove Drive
Pasadena, CA 91102
Attn: Dr. Kenneth Atkins 1
Technical Library 1
Mr. Eugene Pawlik 1
Mr. Dennis Fitzgerald 1

Electro-Optical Systems, Inc.
300 North Halstead
Pasadena, CA 91107
Attn: Mr. R. Worlock 1
Mr. E. James 1
Mr. W. Ramsey 1

Boeing Aerospace Company
P. O. Box 3999
Seattle, WA 98124
Attn: Mr. Donald Grim 1

Intelcom Rad Tech
7650 Convoy Court
P. O. Box 80817
San Diego, CA 92138
Attn: Dr. David Vroom 1

Lockheed Missiles and Space Company
Sunnyvale, CA 94088
Attn: Dr. William L. Owens
Propulsion Systems, Dept. 62-13 1

Fairchild Republic Company
Farmingdale, NY 11735
Attn: Dr. William Guman 1

COMSAT Corporation
950 L'Enfant Plaza S.W.
Washington, DC 20024
Attn: Mr. Sidney O. Metzger 1

Electrotechnical Laboratory
Tahashi Branch
5-4-1 Mukodai-Machi, Tanashi-Shi
Tokyo, JAPAN
Attn: Dr. Katsuva Nakayama 1

Office of Assistant for Study Support
Kirtland Air Force Base
Albuquerque, NM 87117
Attn: Dr. Calvin W. Thomas OAS Ge 1
Dr. Berhart Eber OAS Ge 1

Bell Laboratories
600 Mountain Avenue
Murray Hill, NJ 07974
Attn: Dr. Edward G. Spencer 1
Dr. Paul H. Schmidt 1

Massachusetts Institute of Technology
Lincoln Laboratory
P. O. Box 73
Lexington, MA 02173
Attn: Dr. H. I. Smith 1

Sandia Laboratories
Mail Code 5742
Albuquerque, NM 87115
Attn: Mr. Ralph R. Peters 1

TRW, Inc.
TRW Systems
One Space Park
Redondo Beach, CA 90278
Attn: Mr. M. Huberman 1

Dr. S. Zafran 1

National Aeronautics and Space Administration
Ames Research Center
Moffett Field, CA 94035
Attn: Technical Library 1

National Aeronautics and Space Administration
Langley Research Center
Langley Field Station
Hampton, VA 23365
Attn: Technical Library 1

Hughes Research Laboratories
3011 Malibu Canyon Road
Malibu, CA 90265
Attn: Dr. Jay Hyman 1
Mr. J. H. Molitor 1
Dr. R. L. Poeschel 1
Mr. R. Vahrenkamp 1
Dr. John R. Beattie 1

United States Air Force
Office of Scientific Research
Washington, DC 20025
Attn: Mr. M. Slawsky 1

Princeton University
Princeton, NJ 08540
Attn: Mr. W. F. Von Jaskowsky 1
Dean R. G. Jahn 1
Dr. K. E. Clark 1

Communications Research Centre
Ottawa, Ontario, CANADA
Attn: Dr. W. F. Payne 1

Joint Institute for Laboratory Astrophysics
University of Colorado
Boulder, CO 80302
Attn: Dr. Gordon H. Dunn 1

Department of Aeronautics and Astronautics
Stanford University
Stanford, CA 94305
Attn: Professor Howard S. Seifert 1

Service du Confinement des Plasma
Centre d'Etudes Nucléaires - F.A.R.
B.P. 6
92260 Fontenay-aux-Roses
FRANCE
Attn: Dr. J. F. Bonal 1

International Business Machines Corporation
Thomas J. Watson Research Center
P. O. Box 218
Yorktown Heights, NY 10598
Attn: Dr. Jerome J. Cuomo 1
Dr. James M. E. Harper 1

IBM East Fishkill
D/42K, Bldg. 300-40F
Hopewell Junction, NY 12533
Attn: Dr. Charles M. McKenna 1

DFVLR-Forschungszentrum Braunschweig
Inst. A, Flughafen
3300 Braunschweig
WEST GERMANY
Attn: Dr. H. A. W. Bessling 1

Ion Beam Equipment, Inc.
P. O. Box O
Norwood, NJ 07648
Attn: Dr. W. Laznovsky 1

Optic Electronics Corporation
11477 Pagemill Road
Dallas, TX 75243
Attn: Bill Hermann, Jr. 1

Circuits Processing Apparatus, Inc.
725 Kifer Road
Sunnyvale, CA 94086
Attn: Spencer R. Wilder 1

Ion Tech, Inc.
1807 E. Mulberry
P. O. Box 1388
Fort Collins, CO 80522
Attn: Dr. Gerald C. Isaacson 1

Physicon Corporation
221 Mt. Auburn Street
Cambridge, MA 02138
Attn: H. von Zweck 1

Commonwealth Scientific Corporation
500 Pendleton Street
Alexandria, VA 22314
Attn: George R. Thompson 1

Veeco Instruments Inc.
Terminal Drive
Plainview, NY 11803
Attn: Norman Williams 1

CVC Products
525 Lee Road
P.O. Box 1886
Rochester, N.Y. 14603
Attn: Mr. Georg F. Garfield, Jr.